Constitutive androstane receptor directs T cell adaptation to bile acids in the small intestine

Mei Lan Chen[1,2#], Xiangsheng Huang[3#], Hongtao Wang[3], Courtney Hegner[1,2], Yujin Liu[1], Jinsai Shang[4], Amber Eliason[1], HaJeung Park[5], Blake Frey[6], Guohui Wang[3], Sarah A. Mosure[1,2,4], Laura A. Solt[1,4], Douglas J. Kojetin[4,7], Alex Rodriguez-Palacios[8,9], Deborah A. Schady[10], Casey T. Weaver[6], Matthew E. Pipkin[1], David D. Moore[11]*, and Mark S. Sundrud[1]*

[1]Department of Immunology and Microbiology, The Scripps Research Institute, Jupiter, FL 33458, USA

[2]Skaggs Graduate School of Chemical and Biological Sciences, The Scripps Research Institute, Jupiter, FL, 33458, USA.

[3]Department of Pediatrics, Section of Gastroenterology, Baylor College of Medicine and Texas Children's Hospital, Houston, TX, 77030, USA

[4]Department of Integrative Structural and Computational Biology, The Scripps Research Institute, Jupiter, FL 33458, USA

[5]X-ray Crystallography Core Facility, The Scripps Research Institute, Jupiter, FL 33458, USA

[6]Department of Pathology, University of Alabama at Birmingham, Birmingham, AL 35203, USA

[7]Department of Molecular Medicine, The Scripps Research Institute, Jupiter, FL 33458, USA

[8]Division of Gastroenterology and Liver Disease, School of Medicine, Case Western Reserve University, Cleveland, Ohio 44106, USA

[9]University Hospitals Research and Education Institute, University Hospitals Cleveland Medical Center, Cleveland, Ohio 44106, USA

[10]Department of Pathology and Immunology, Texas Children's Hospital, Baylor College of Medicine, Houston, TX, 77030, USA.

[11]Department of Molecular and Cellular Biology, Baylor College of Medicine, 1 Baylor Plaza, Houston, Texas 77030, USA

[#]Equal contribution

*Correspondence: David D. Moore (moore@bcm.edu), Mark S. Sundrud (msundrud@scripps.edu)

Key words: IBD, T cells, Th1, Th17, bile acids, MDR1, CAR, NR1I3, xenobiotics

Abbreviations: MDR1, multidrug resistance 1; TNFα, tumor necrosis factor alpha; IFNγ, interferon gamma; IL-10, interleukin-10; IL-17, interleukin-17; TCR, T cell receptor; *Abcb1a*, ATP-binding cassette subfamily B, member 1a; *Abcb1b*, ATP-binding cassette subfamily B, member 1b; *Rag1*, recombination-activating gene 1; *Rag2*, recombination-activating gene 2.

Bile acids (BAs) are fundamental lipid emulsifying metabolites synthesized in hepatocytes and maintained *in vivo* through enterohepatic circulation between the liver and small intestine[1]. As detergents, BAs can cause toxicity and inflammation in enterohepatic tissues[2], and several nuclear receptors have evolved to detoxify BAs in hepatocytes and enterocytes[3]. By contrast, it is unclear how mucosal immune cells protect themselves from high BA concentrations in the small intestine. We previously reported that CD4$^+$ T effector (Teff) cells upregulate expression of the xenobiotic transporter MDR1 in the ileum to prevent BA toxicity and suppress Crohn's disease-like small bowel inflammation[4]. Here, we identify the nuclear xenobiotic receptor, constitutive androstane receptor (CAR/*NR1I3*), as a transcriptional regulator of MDR1 expression in mucosal T cells. CAR promoted large-scale transcriptional reprogramming in Teff cells infiltrating the small intestine lamina propria (siLP), but not the colon. CAR activation by non-BA components in bile not only induced expression of detoxifying enzymes and transporters in siLP T cells, as in hepatocytes, but also the key anti-inflammatory cytokine, *Il10*. Accordingly, CAR-deficiency in T cells exacerbated, whereas pharmacologic CAR activation suppressed, BA-driven ileitis in T cell-reconstituted *Rag*$^{-/-}$ mice. These data suggest that CAR acts locally in small intestinal T cells to direct a unique transcriptional response that detoxifies BAs and fosters inflammation-resolution. Pharmacologic activation of this program offers an unexpected strategy to treat small bowel Crohn's disease.

In seeking to define transcriptional mechanisms that promote MDR1 upregulation in siLP Teff cells to safeguard small bowel immune homeostasis in the presence of BAs[4], we considered the ligand-regulated nuclear receptors (NRs), which act as environmental sensors to regulate diverse gene expression programs important for immunity, inflammation, metabolism and gastrointestinal physiology[5]. To test the contribution of each of the 49 mouse NRs to MDR1 regulation in siLP Teff cells, we performed a pooled *in vivo* RNAi screen using MDR1-dependent rhodamine 123 (Rh123) efflux[6] as a readout. Naïve CD4$^+$ T cells on the FVB/N (FVB) background were activated and transduced *in vitro* with a library of 258 mouse retroviruses carrying shRNAmirs against 70 genes together with the fluorescent reporter, ametrine (**Fig. 1a**). In addition to NRs, this library included shRNAmirs against 10 major NR co-activators and co-repressors, the aryl hydrocarbon receptor (AhR), the cell-surface BA receptor Takeda G-coupled protein receptor 5 (Tgr5; encoded by *Gpbar1*)[7] and its downstream transcription factor (*Creb1*), as well as a number of positive (*Abcb1a*, *Abcb1b*) and negative (*Cd8a*, *Cd19*, *EGFP*, *RFP*) control genes (Supplemental Table 1). Separately-transduced T cells were pooled, FACS-sorted for ametrine expression and transplanted into syngeneic *Rag1*$^{-/-}$ mice. Six-weeks later, transduced Teff cells were recovered by FACS-sorting from spleen or siLP, and portions of these cells

were sub-divided into MDR1^{hi} or MDR1^{lo} subsets based on *ex vivo* Rh123 efflux; relative shRNAmir abundances within each cell pool were quantified by DNA-seq (**Fig. 1a**).

Three sets of shRNAmirs—against thyroid hormone receptor alpha (*Thra*), estrogen related receptor alpha (*Esrra*), and constitutive androstane receptor (CAR/*Nr1i3*)—were most strongly and consistently enriched in MDR1^{lo} *vs*. MDR1^{hi} Teff cells from both spleen and siLP, similar to shRNAmirs against MDR1 (*Abcb1a*) itself, and after excluding 36 shRNAmirs that either markedly reduced Teff cell persistence *in vivo* or that were poorly represented (before and after *in vivo* transfer) (**Fig. 1b**; Extended Data Fig. 1a-b). This suggested that *Thra, Esrra* and CAR/*Nrli3* might each be positive regulators of MDR1 expression, although none have known functions in T cells. We prioritized CAR for validation because of its reported roles in protecting hepatocytes from drug- and BA-induced toxicity[8], which include promoting hepatic MDR1 expression[9]. Individual shRNAmir expression experiments confirmed that 3 of the 5 shRNAmirs against CAR reduced MDR1-dependent Rh123 efflux in Teff cells recovered from transferred *Rag1*$^{-/-}$ mice (**Fig. 1c**, Extended Data Fig. 1c-d). These same three constructs diminished MDR1 (*Abcb1a*) and CAR (*Nr1i3*) gene expression, as judged by qPCR, as well as expression of the signature CAR transcriptional target gene, *Cyp2b10*[10] (Extended Data Fig. 1e).

CAR binds to DNA and regulates transcription as a heterodimer with retinoid X receptors (RXRα/β/γ)[11]. However, RXRs also dimerize with many other NRs, including retinoic acid receptors (RARα/β/γ), peroxisome proliferator-activated receptors (PPARα/δ/γ) and vitamin D receptor (VDR), all of which regulate diverse aspects of T cell function *in vivo*. Consistent with this broader function of RXRs, shRNAmir-mediated depletion of RXRα—the major RXR isoform expressed in T cells—did not selectively regulate MDR1 expression in mucosal T cells, but rather impaired the persistence of circulating Teff cells (Extended Data Fig. 1f). Depletion of the CAR-related xenobiotic-sensor, pregnane X receptor (PXR)[12], influenced neither mucosal MDR1 expression nor Teff cell persistence *in vivo* (**Fig. 1b**; Extended Data Fig. 1f). In line with this result, Teff cells from C57BL/6 (B6)-derived CAR-deficient (*Nr1i3*$^{-/-}$) mice displayed lower MDR1 expression and function than those from PXR-deficient (*Nr1i2*$^{-/-}$) mice, after co-transfer into *Rag1*$^{-/-}$ mice together with CD45.1 wild type cells; Teff cells lacking both CAR and PXR showed equivalently low MDR1 expression and function as those lacking only CAR (Extended Data Fig. 1g-i). These data implicate CAR in the regulation of mucosal T cell function *in vivo*.

shRNAmir-mediated CAR depletion in FVB wild type T cells exacerbated T cell transfer-induced weight loss in *Rag1*$^{-/-}$ mice, and did so in a manner that correlated directly with the degree of MDR1 down-regulation in these cells (**Fig. 1d-e**; Extended data Fig. 1c-d). This result was consistent

with our prior studies showing that transfer of FVB T cells lacking MDR1 (*Abcb1a*$^{-/-}$*Abcb1b*$^{-/-}$) into syngeneic *Rag1*$^{-/-}$ mice produces more severe weight loss than that of wild type counterparts—due to induction of both colitis and BA-driven ileitis[4]—and is distinct from wild type naïve CD4^{+} T cells, which induce only colitis in immunodeficient hosts[13]. Naive T cells from B6-derived CAR-null (*Nr1i3*$^{-/-}$) mice also precipitated more severe weight loss and ileitis, but equivalent colitis, compared with wild type counterparts, after transfer into *Rag2*$^{-/-}$ mice that were co-housed to normalize microflora (**Fig. 1f-h**). Therapeutic administration of the BA sequestering resin, cholestyramine (CME)[14], which binds BAs in the lumen of the small intestine and prevents reabsorption into the ileal mucosa, normalized weight loss and ileitis between *Rag2*$^{-/-}$ mice receiving CAR-sufficient or CAR-deficient T cells (Extended Data Fig. 2a-b); as did ablation of the ileal BA reuptake transporter, Apical sodium-dependent BA transporter (Asbt/*Slc10a2*)[15] in *Rag1*$^{-/-}$ T cell recipients (Extended Data Fig. 2c-d). Neither genetic nor pharmacological inhibition of ileal BA reabsorption affected the severity of T cell transfer-induced colitis (Extended Data Fig. 2b, 2d). These results suggest that CAR acts in T cells selectively to promote small bowel immune homeostasis, and that loss of CAR in T cells exacerbates ileitis that is not transmissible by microbiota and requires BA reabsorption.

To elucidate CAR-dependent transcriptional programs in mucosal T cells, we used RNA-seq to analyze the transcriptomes of wild type and CAR-deficient Teff cells from spleen, siLP and colon lamina propria (cLP) of congenically co-transferred *Rag1*$^{-/-}$ mice—where CD45.1 CAR-sufficient and CD45.2 CAR-deficient Teff cells were present as tissue bystanders in the same animals (**Fig. 2a**). Wild type Teff cell gene expression differed substantially in spleen, siLP and cLP, whereas CAR-deficiency most conspicuously altered T cell gene expression in siLP (**Fig. 2b**). siLP Teff cells lacking CAR failed to upregulate dozens of 'siLP-signature' genes (*i.e.*, genes increased in wild type siLP Teff cells, compared to those from either spleen or colon), and acquired transcriptional features of wild type Teff cells from the colon (**Fig. 2c-d**). CAR-dependent siLP-signature genes included chaperones, receptors and enzymes involved in lipid binding, transport and metabolism (*e.g.*, *Apold1*, *Pex26*, *Dgkh*, *Ldlr*, *Phyhd1*, *Lclat1*; **Fig. 2c**), and were enriched for genes previously found to be induced by CAR in mouse hepatocytes, by RNA-seq, after *in vivo* administration of the synthetic CAR agonist ligand, 1,4-*Bis*(3,5-Dichloro-2-pyridinyloxy) benzene (TCPOBOP, or simply TC)[16] (Extended Data Fig. 3a-b). Genes displaying CAR-dependent expression in both siLP Teff cells and hepatocytes were enriched for loci at which TC-inducible binding of a GFP-tagged mouse CAR protein was previously determined in hepatocytes by ChIP-seq[17] (Extended Data Fig. 3c). As expected, these presumed CAR target genes included MDR1/*Abcb1a* and *Cyp2b10*, but also other ABC-family transporters (*e.g.*, *Abcb4*) and cytochrome P450 enzymes (*e.g.*, *Cyp2r1*) (Extended Data Fig. 3d), consistent with induction of a BA detoxification

program. CAR-deficient Teff cells showed reduced persistence in reconstituted *Rag1*$^{-/-}$ mice, relative to co-transferred CD45.1 wild type cells; this was most pronounced in siLP (Extended Data Fig. 4a-c), and trended towards being rescued by ablation of Asbt-dependent BA reabsorption in *Rag1*$^{-/-}$ recipients (Extended Data Fig. 4d-f).

Preferential CAR activity in mouse siLP Teff cells suggested that CAR might also regulate human T cell function in the small intestine. Therefore, we analyzed the expression and function of CAR in human peripheral blood T cell subsets expressing the small bowel-homing receptors, α4β7 integrin and CCR9[18], which are more likely to have recently recirculated from the intestinal mucosa. A small but reliable subset of α4^{+}β7^{+}CCR9^{+} Teff cells (~ 1-5%) was detected in peripheral blood of healthy adult donors (Extended Data Fig. 5a-c). Expression of these receptors was absent on naïve CD4^{+} T cells, as expected, and reduced among circulating CD25^{+} T regulatory (Treg) cells (Extended Data Fig. 5a-c), suggesting that Treg cells may be more efficiently retained in the intestinal mucosa than Teff cells. Given the lack of specific CAR antibodies, we assessed CAR expression and function based on predicted transcriptional outputs, beginning with MDR1. MDR1-dependent Rh123 efflux was undetectable in circulating CD4^{+} naïve and Treg cells, but increased progressively as human Teff cells acquired expression of α4 integrin, β7 integrin, and CCR9 (Extended Data Fig. 5d-e). α4^{+}β7^{+}CCR9^{+} Teff cells also displayed increased *ex vivo* expression of *ABCB1*, as judged by qPCR, as well as of CAR (*NR1I3*) and *CYP2B6*—the human ortholog of mouse *Cyp2b10* and hallmark CAR transcriptional target[19]—compared with naïve, Treg or α4^{-}β7^{-}CCR9^{-} Teff cells (Extended Data Fig. 5f). Most importantly, only α4^{+}β7^{+}CCR9^{+} Teff cells responded to *ex vivo* treatment with the human CAR agonist ligand, 6-(4-Chlorophenyl)imidazo[2,1-b][1,3]thiazole-5-carbaldehyde O-(3,4-dichlorobenzyl) oxime (CITCO)[19] by upregulating *CYP2B6* and *ABCB1* (Extended Data Fig. 5g-h). α4^{+}β7^{+}CCR9^{+} Teff cells were enriched for CCR6^{+}CXCR3^{hi}CCR4^{lo} "Th17.1" cells (Extended Data Fig. 5i-l), which display both Th17 and Th1 effector functions, as well as elevated MDR1 expression[20]. Nonetheless, combined expression of α4 integrin, β7 integrin, and CCR9 increased the proportion of MDR1-expressing Th17.1 cells, as well as of MDR1-expressing Th17 (CCR6^{+}CXCR3^{lo}CCR4^{hi}) and Th1 (CCR6^{-}CXCR3^{hi}CCR4^{lo}) cells, compared with lineage counterparts lacking one or more small bowel-homing receptors (Extended Data Fig. 5m-n). These data suggest that CAR is preferentially active in both mouse and human small intestinal Teff cells.

Enhanced CAR function in siLP Teff cells could involve local activation by endogenous metabolites. Consistent with this possibility, bile (from gallbladder), as well as sterile, soluble small intestine lumen content (siLC) from wild type B6 mice—but not colon lumen content (cLC) or serum—

induced *Abcb1a* and *Cyp2b10* upregulation in *ex vivo*-stimulated wild type, but not CAR-deficient, Teff cells from spleens of reconstituted *Rag1*$^{-/-}$ mice (**Fig. 2e**; Extended Data Fig. 6a). CAR-dependent gene expression in this *ex vivo* culture system was also induced by TC, inhibited by the CAR inverse agonist, 5α-Androstan-3β-ol[8], and unaffected by the PXR agonist, 5-Pregnen-3β-ol-20-one-16α-carbonitrile (PCN)[12] (**Fig. 2e**; Extended Data Fig. 6a). The same dilutions of bile and siLC that enhanced CAR-dependent gene expression in Teff cells also promoted recruitment of a co-activator peptide (PGC1α) to recombinant CAR-RXRα ligand-binding domain (LBD) heterodimers, but not to RXRα LBD homodimers, in time-resolved fluorescence resonance energy transfer (TR-FRET) experiments (**Fig. 2f-g**; Extended Data Fig. 7a-b). Since CAR is thought to indirectly sense, but not directly bind, major BA species[21], these data suggested that components of bile other than BAs might activate the CAR LBD; bile consists of mixed micelles containing BAs, phospholipids, cholesterol, fatty acids and bile pigments (*e.g.*, bilirubin)[1]. Consistent with a BA-independent mechanism of CAR activation, siLC-mediated CAR-RXRα LBD heterodimer activation was not affected by CME-mediated depletion of free BAs (Extended Data Fig. 7c), and no major primary or secondary BA species was sufficient to activate CAR-RXRα LBD heterodimers in TR-FRET experiments, or to stimulate CAR-dependent gene expression in *ex vivo*-cultured Teff cells (Extended Data Fig. 7d, data not shown). CAR-RXRα LBD heterodimers were also activated by siLC from germ-free (GF) wild type mice (Extended Data Fig. 7c, data not shown). Thus, host-derived, non-BA constituents of bile may directly enhance CAR transcriptional activity in siLP Teff cells.

To further explore CAR immunoregulatory functions, we used gene set enrichment analysis (GSEA) to examine the impact of CAR-deficiency on gene expression previously associated with major pro- and anti-inflammatory T helper cell lineages. Unexpectedly, siLP Teff cells lacking CAR displayed reduced gene expression ascribed to type 1 regulatory (Tr1) cells[22], a key subset of Foxp3^{-}IL-10^{+} T cells recognized for suppressing mucosal inflammation in humans and mice (**Fig. 3a-c**)[23]. Consistent with this, CAR was strictly required for the expression of both a Thy1.1-expressing *Il10*-reporter allele[24] (10BiT; **Fig. 3d-e**) and endogenous IL-10 protein (Extended Data Fig. 8a-e) in Teff cells re-isolated from transferred *Rag1*$^{-/-}$ mice. Conversely, TC, as well as bile and siLC from wild type mice, induced CAR-dependent *Il10* upregulation in *ex vivo*-stimulated Teff cells (**Fig. 3f**; Extended Data Fig. 6), akin to *Abcb1a* and *Cyp2b10* (**Fig. 2e**). Colon lumen content acted on both wild type and CAR-deficient Teff cells to enhance *Il10* expression (**Fig. 3f**), suggesting that non-overlapping CAR-dependent and CAR-independent pathways may modulate *Il10* expression in mucosal T cells in the small and large intestines, respectively. CAR-dependent IL-10 expression in the *Rag1*$^{-/-}$ T cell transfer model was transient—

peaking 2-weeks after T cell engraftment and waning thereafter—and followed the kinetics of both T cell infiltration into siLP and *ex vivo* CAR (*Nr1i3*), MDR1 (*Abcb1a*) and *Cyp2b10* gene expression (Extended Data Fig. 8f-h). CAR was also required for IL-10 expression in endogenous siLP effector and regulatory T cell subsets from intact mice, but only after injection of soluble anti-CD3 antibodies to induce acute intestinal inflammation[23] (Extended data Figure 9a-c). In addition, CAR/*Nr1i3* expression was upregulated during the *in vitro* development of Tr1 cells, where naïve $CD4^+$ T cells were activated and expanded in the combined presence of IL-27—a cytokine that promotes Stat3-dependent IL-10 expression[22]—and the synthetic corticosteroid, dexamethasone[25] (**Fig. 3g**). Loss of CAR restricted IL-10 production by these *in vitro*-polarized Tr1 cells (**Fig. 3h-i**). By contrast, CAR expression was not induced during the *in vitro* development of other conventional effector (*e.g.*, Th1, Th2, Th17) or regulatory (*e.g.*, induced (i)Treg) lineages, compared with naïve T cells, and loss of CAR had no bearing on the *in vitro* development of these cells (**Fig. 3g**, Supplemental Table 2). These data reveal a novel and essential function for CAR in *Il10* gene regulation, whether direct or indirect, which may synergize with the CAR-dependent BA detoxification program in mucosal T cells to foster resolution of small bowel inflammation.

Gene expression associated with Th17 cells—an important lineage of $ROR\gamma t^+$ pro-inflammatory T cells implicated in the pathogenesis of inflammatory bowel diseases[26]—was reciprocally increased in siLP Teff cells lacking CAR (**Fig. 3b**), and reduced IL-10 expression in Teff cells lacking CAR paralleled their accumulation as $ROR\gamma t^+IL\text{-}17A^-$ 'poised' Th17 cells[27,28] in siLP of transferred *Rag1*$^{-/-}$ mice (Extended Data Fig. 9d-e). However, this phenotype was recapitulated by *Il10*$^{-/-}$ Teff cells replete for CAR (Extended Data Fig. 9f-g), suggesting that CAR might suppress the development and/or accumulation of mucosal Th17 cells indirectly, via IL-10 induction. Other effector and regulatory T cell gene signatures were unaffected by loss of CAR *in vivo* (**Fig. 3b**).

Finally, we reasoned that if CAR-deficiency in Teff cells exacerbates BA-driven small bowel inflammation, pharmacologic CAR activation might be protective. A single administration of the selective CAR agonist, TC, to *Rag1*$^{-/-}$ mice reconstituted with a mixture of CD45.1 wild type and CD45.2 CAR-deficient T cells was sufficient to induce *Abcb1a*, *Cyp2b10* and *Il10* upregulation in wild type, but not CAR-deficient, Teff cells within 72 hr (**Fig. 4a**). Weekly TC administration reduced ileitis, but not colitis, in *Rag2*$^{-/-}$ mice reconstituted with only wild type T cells and fed a standard 0.2% cholic acid (CA)-supplemented diet to increase the size of the circulating BA pool and promote small bowel injury[28] (**Fig. 4b-c**); CA-feeding increased morbidity and mortality in *Rag2*$^{-/-}$ mice receiving wild type T cells, but had no obvious effects on *Rag2*$^{-/-}$ mice in the absence of T cell transfer (**Fig. 4b**, data not shown). As

expected, therapeutic effects of TC were abolished in CA-fed *Rag2*$^{-/-}$ mice reconstituted with CAR-deficient T cells (Extended Data Fig. 10). These data suggest that BA-supplementation promotes, whereas CAR activation in T cells suppresses, experimental ileitis. Although additional effects of TC-mediated CAR activation in parenchymal tissues could not be discerned from these studies, the results reveal an unexpected new strategy for the treatment of small bowel Crohn's disease.

BAs have emerged as important and pleotropic signaling metabolites that have both pro- and anti-inflammatory effects in the gastrointestinal tract via dynamic interactions with germline-encoded host receptors and the microbiota[1]. Whereas low (micromolar) concentrations of secondary BAs in the colon—produced via bacterial metabolism—appear to support mucosal immune tolerance by activating and expanding colonic Foxp3^{+} Treg cells[29,30], the higher (millimolar) concentrations of primary BAs present in the small intestine—due to active reuptake during enterohepatic circulation—may be more pro-inflammatory and cytotoxic. Our study suggests that the BA- and xenobiotic-sensing nuclear receptor, CAR/Nr1i3, reprograms mucosal T cell gene expression in the small intestine to counter BA-induced toxicity and inflammation (**Fig. 4d**). The additional contribution of non-BA components in bile to CAR activation in small intestinal T cells suggests more direct, extensive and compartmentalized interplay between mucosal T cells and hepatic metabolism than previously recognized. Pharmacologic CAR activation not only offers a new and more targeted approach to treat small bowel Crohn's disease; it also opens new avenues for exploring lymphocyte specialization across the intestinal tract.

Experimental procedures

Mice

C57BL/6 (B6)-derived wild type (Stock No: 000664), CD45.1 (Stock No: 002014), *Rag1*$^{-/-}$ (Stock No: 002216), *Rag2*$^{-/-}$ (Stock No: 008449) and *Il10*$^{-/-}$ (Stock No: 004368) mice were purchased from The Jackson Laboratory. Wild type FVB/N mice were purchased from Taconic. B6-derived *Nr1i2*$^{-/-}$, *Nr1i3*$^{-/-}$ and *Nri12*$^{-/-}$*Nr1i3*$^{-/-}$ mice were provided by D. Moore (Baylor College of Medicine, BCM). FVB-derived *Rag1*$^{-/-}$ mice were a gift of Dr. Allan Bieber (Mayo Clinic, Rochester, MN). B6-derived BAC *Il10*-Thy1.1 transgenic reporter (10BiT) mice were provided by C. Weaver (University of Alabama-Birmingham, UAB) and have been described previously[24]. B6-derived *Rag1*$^{-/-}$ mice were crossed with *Slc10a2*$^{-/-}$ mice (gift of Dr. Paul Dawson, Emory University) in the Sundrud lab to generate *Rag1*$^{-/-}$ mice lacking the Asbt transporter as in[4]. Lumen contents (colon, small intestine) were harvested (see below)

from specific pathogen-free (SPF) or germ-free wild type B6 mice housed at the University of Alabama-Birmingham (UAB; courtesy of Dr. Weaver). All breeding and experimental use of animals was conducted in accordance with protocols approved by IACUC committees at Scripps Florida, BCM or UAB.

Human blood samples

Human blood samples were collected and analyzed in accordance with protocols approved by Institutional Review Boards at Scripps Florida and OneBlood (Orlando, Florida). Blood was obtained following informed written consent, and consenting volunteers willingly shared clinical history and demographic information prior to phlebotomy. Institutional Review Boards at OneBlood and Scripps Florida approved all procedures and forms used in obtaining informed consent, and all documentation for consenting volunteers is stored at OneBlood.

$CD4^+$ T cell isolation and culture

Purified $CD4^+CD25^-$ T cells were magnetically isolated from spleen and peripheral lymph node mononuclear cells using an EasySep magnetic T cell negative isolation kit (Stem Cell Technologies, Inc.) with addition of a biotin anti-mouse CD25 antibody (0.5 µg/mL; BioLegend). Magnetically-enriched $CD4^+$ T cells were cultured in (DMEM) supplemented with 10% heat-inactivated fetal bovine serum, 2mM L-glutamine (Gibco), 50uM 2-mercaptoethanol (Amresco), 1% MEM vitamin solution (Gibco), 1% MEM non-essential amino acids solution(Gibco), 1% Sodium Pyruvate(Gibco), 1% Arg/Asp/Folic acid (Gibco), 1% HEPES (Gibco), 0.1% gentamicin (Gibco) and 100u/ml Pen-Strep (Gibco). For *Rag1*$^{-/-}$ transfer experiments, magnetically enriched $CD4^+CD25^-$ T cells were FACS-sorted to obtain pure naïve T cells ($CD3^+CD4^+CD25^-CD62L^{hi}CD44^{lo}$). For *ex vivo* isolation of mononuclear cells from tissues of T cell-reconstituted Rag-deficient mice, single cell suspensions were prepared from spleen, peripheral lymph nodes, or mesenteric lymph nodes (MLN) by mechanical disruption passing through 70 µm nylon filters (BD Biosciences). For intestinal tissues, small intestines and colons were removed, rinsed thoroughly with PBS to remove the fecal contents, and opened longitudinally; Peyer's patches were removed from small intestines. Tissues were incubated for 30 minutes at room temperature in DMEM media without phenol red (Genesee Scientific) plus 0.15% DTT (Sigma-Aldrich) to eliminate mucus layer. After washing with media, intestines were incubated for 30 minutes at room temperature in media containing 1 mM EDTA (Amresco) to remove the epithelium. Intestinal tissue was digested in media containing 0.25 mg/mL liberase TL (Roche) and 10 U/mL RNase-free DNaseI (Roche) for 15-25

minutes at 37 °C. Lymphocyte fractions were obtained by 70/30% Percoll density gradient centrifugation (Sigma-Aldrich). Mononuclear cells were washed in complete T cell media and resuspended for downstream FACS analysis or sorting.

Naïve CD4$^+$ T cell activation and polarization: magnetically enriched CD4$^+$CD25$^-$ T cells were seeded (at 4x10^5 cells/cm^2 and 1x10^6 cells/mL) in 96- or 24-well flat bottom plates pre-coated for 1-2 hr at 37 °C with goat-anti-hamster whole IgG (50 µg/mL; Invitrogen). Activation was induced by adding hamster-anti-mouse CD3ε (0.3 or 1 µg/mL; BioLegend) and hamster-anti-mouse CD28 (0.25 or 0.5 µg/mL; BioXcell). After 48 hr, cells were removed from coated wells and re-cultured at 1x10^6 cells/mL in media with or without 10 U/mL recombinant human IL-2 (rhIL-2) (NIH Biorepository), depending on the experiment (see below). For polarization studies, cells were activated in the presence of the following sets of cytokines and/or neutralizing antibodies (all from R&D Systems): Th0—media alone; Th1—recombinant human (rh)IL-12 (5 ng/mL) plus anti-mouse IL-4 (5 µg/mL); Th2—rhIL-4 (10 ng/mL) plus anti-mouse IFNγ (5 µg/mL); non-pathogenic (np)Th17—recombinant mouse (rm)IL-6 (40 ng/mL) plus rhTGFβ1 (1 ng/mL), anti-mouse IFNγ (5 µg/mL) and anti-mouse IL-4 (5 µg/mL); pathogenic (p)Th17— rmIL-6 (40 ng/mL) plus rhTGFβ1 (1 ng/mL), rhIL-23 (10 ng/mL) anti-mouse IFNγ (5 µg/mL) and anti-mouse IL-4 (5 µg/mL); induced T regulatory (i)Treg—rhTGFβ1 (5 ng/mL) plus rhIL-2 (10 U/mL), anti-mouse IFNγ (5 µg/mL) and anti-mouse IL-4 (5 µg/mL). For Tr1 cultures, cells were activated in the presence of rhIL-27 (100 ng/mL) and/or dexamethasone (100 nM; Sigma-Aldrich). Cytokine, antibodies and/or Dex were added at the time of activation (day 0), and re-added to expansion media between days 2-4 of culture. Cells were analyzed for intracellular expression of transcription factors and/or cytokines, to confirm polarization, on day 4 after re-stimulation with phorbol 12-myrisate 13-acetate (PMA; 10nM; Life Technologies) and ionomycin (1uM; Sigma-Aldrich) for 3-4 hr in the presence of brefeldin A (BFA; 10ug/mL; Life Technologies).

Ex vivo-stimulation of FACS-sorted effector/memory (Teff) cells from reconstituted Rag1$^{-/-}$ mice: 30,000 CD45.1 (wild type) or CD45.2 (*Nr1i3*$^{-/-}$) cells—FACS-purified from spleens of B6.*Rag1*$^{-/-}$ 2-3 weeks post naïve T cell transfer—were activated in round-bottom 96-well plates with mouse anti-CD3/anti-CD28 T cell expander beads (1 bead/cell; Life Technologies) in complete media containing 10 U/mL recombinant human (rh) IL-2 for 24 hr in the presence or absence of synthetic or endogenous CAR agonists (see 'compound and tissue extracts' below).

Retroviral plasmids and transductions

shRNAmirs against mouse nuclear receptors were purchased (TransOMIC) or custom synthesized using the shERWOOD algorithm[41]. For cloning into an ametrine-expressing murine retroviral vector (LMPd) containing the enhanced miR-30 cassette[42,43], shRNAmirs were PCR amplified using forward (5′-AGAAGGCTCGAGAAGGTATATTGC-3′) and reverse (5′-GCTCGAATTCTAGCCCCTTGAAGTC CGAGG-3′) primers containing XhoI and EcoR1 restriction sites, respectively. All retroviral constructs were confirmed by sequencing prior to use in cell culture experiments. Retroviral particles were produced by transfection of Platinum E (PLAT-E) cells with the TransIT-LT1 transfection reagent (Mirus) in Opti-MEM I reduced serum medium. Viral supernatants containing 10 μg/mL polybrene were used to transduce $CD4^+CD25^-$ T cells 24 hr post-activation (anti-CD3/anti-CD28; as above). Transductions were enhanced by centrifugation at 2000 rpm for 1 hr at room temperature, and incubation at 37 °C until 48 hr post-activation. Transduced cells were expanded in complete media containing 10 U/mL rhIL-2.

Cell lines

PLAT-E cells, derived from the HEK-293 human embryonic kidney fibroblasts and engineered for improved retroviral packaging efficiency, were provided by M. Pipkin (Scripps Florida). All cell lines were tested to be mycoplasma free, and cultured in DMEM plus 10% FBS, 2 mM L-glutamine, 50 uM 2-mercaptoethanol, 1% HEPES, 0.1% gentamicin and 100u/ml Pen-Strep.

T cell transfer colitis

For experiments using B6-derived wild-type or CAR-deficient (*Nr1i3*$^{-/-}$) T cells, 0.5 x 10^6 FACS-sorted naïve T cells (sorted as $CD4^+CD25^-CD62L^{hi}CD44^{lo}$ at Scripps Florida; $CD4^+CD45RB^{hi}$ at BCM) were injected intraperitoneally (i.p.) into syngeneic *Rag1*$^{-/-}$ (at Scripps Florida) or *Rag2*$^{-/-}$ (at BCM) recipients and analyzed between 2-6 weeks post-transfer. For mixed congenic T cell transfers, FACS-purified naïve T cells ($CD4^+CD25^-CD62L^{hi}CD44^{lo}$) from CD45.1 wild type and CD45.2 CAR-deficient (*Nr1i3*$^{-/-}$), PXR-deficient (*Nr1i2*$^{-/-}$), CAR- and PXR-deficient (*Nri12*$^{-/-}$*Nr1i3*$^{-/-}$) or *Il10*$^{-/-}$ mice were mixed in a 1:1: ratio and transferred together (0.5 x 10^6 total cells). For transfers of shRNAmir-expressing T cells, magnetically enriched $CD4^+CD25^-$ T cells from FVB/N (FVB) wild-type mice, activated and transduced as above, were expanded until day 5 in media containing rhIL-2 and transferred into syngeneic *Rag1*$^{-/-}$ mice (0.5 x 10^6 total cells). All *Rag1*$^{-/-}$ recipients were weighed immediately prior to T cell transfer to determine baseline weight, and then weighed twice weekly after T cell transfer for the duration of the experiment. Mouse chow diets containing 2% Cholestyramine (CME) (Sigma-Aldrich) or 0.2% Cholic

Acid (CA) (Sigma-Aldrich) and control diets were custom made (Teklad Envigo, Madison, WI) and fed to mice as follows: CME-supplemented diets were started 3 weeks after T cell transfer and continued for 3 weeks; cholic acid diet was started within 3 days post-T cell transfer and continued for 6 weeks (or until mice died). TCPOBOP (TC; Sigma-Aldrich) was initially reconstituted in sterile DMSO, stored at -20 ºC, and diluted in sterile saline and sonicated immediately prior to injections. 3 mg/kg TC was injected intra-peritoneal (i.p.) weekly as indicated. Transferred *Rag1*$^{-/-}$ or *Rag2*$^{-/-}$ mice were euthanized upon losing 20% of pre-transfer baseline weight. All *Rag*$^{-/-}$ mice receiving different donor T cell genotypes were co-housed to normalize microflora exposure.

Anti-CD3-induced intestinal injury

Wild-type (B6) or CAR-deficient (B6.*Nr1i3*$^{-/-}$) mice were injected i.p. with 15 ug of soluble, Ultra-LEAF purified anti-CD3 (clone: 145-2C11) or IgG isotype control (clone: HTK888) (BioLegend) twice over 48 hr. Animals were euthanized, and T cells analyzed 4 hr after the second injection.

Histology

Colon (proximal, distal) or small intestine (proximal, mid, distal/ileum) sections (~ 1 cm) were cut from euthanized *Rag1*$^{-/-}$ or *Rag2*$^{-/-}$ mice 6 weeks post-T cell transfer. In some experiments, 10 cm segments of distal small intestine and whole colon were dissected from mice and fixed intact. All tissues were fixed in 10% neutral buffered formalin, embedded into paraffin blocks, cut for slides at 4-5 microns, and stained with hematoxylin and eosin (H&E). H&E-stained sections were analyzed and scored blindly by a pathologist with GI expertise using an Olympus BX41 microscope and imaged using an Olympus DP71 camera. Colons and ilea were histologically graded for inflammation severity using a combination of previously-reported grading models published by Kim, et al.[31] and by Berg et al.[32]. The scheme published by Kim, et al grades 5 different descriptors which include crypt architecture (normal, 0 - severe crypt distortion with loss of entire crypts, 3), degree of inflammatory cell infiltration (normal, 0 – dense inflammatory infiltrate, 3), muscle thickening (base of crypt sits on the muscularis mucosae, 0 - marked muscle thickening present, 3), goblet cell depletion (absent, 0- present, 1) and crypt abscess (absent, 0-present, 1). Berg et al uses a grade 0 through 4 model of overall severity with grade 1 being normal and grade 4 showing diffuse intestinal involvement with transmural inflammation, marked epithelial hyperplasia, marked mucin depletion with abscesses and ulcers.

Flow cytometry

Cell surface and intracellular FACS stains were performed at 4 ºC for 30 minutes, washed with phosphate buffered saline (PBS) and acquired on a flow cytometer. Analysis of Rh123 efflux was performed as in[4]. Background Rh123 efflux was determined by the addition of the MDR1 antagonist, elacridar (10 nM), to Rh123-labelled cells prior to the 37 ºC efflux step. Anti-mouse antibodies used for FACS analysis included: Alexa Fluor 700 anti-CD45, APC anti-CD45.1, BV711 anti-CD4, BV510 anti-CD25, BV650 anti-CD3, Percp-Cy5.5 anti-CD62L, PE-CY7 anti-CD44, BV605 anti-CD62L, PE anti-α4β7, Alexa Fluor700 anti-CD4, FITC anti-CD44, BV421 anti-CD44, e450 anti FOXP3, BV605 anti-TNF, Percp-Cy5.5 anti-Il-17a, BV711 anti-INFγ, PE anti-Il-4, PE-CY7 anti-IL-10, PE anti-Thy1.1, FITC anti-CD3, Percp-Cy5.5 anti-Thy1.1, PE anti-CD3, PE anti-TCRβ, APC anti-INFg, FITC anti-CD45.2, PE anti-α4β7 (from BioLegend); and BUV395 anti-CD3, PE-CF594 anti-CD25, FITC anti-Ki-67, PE-CF594 anti-RORγt (from BD). Anti-human antibodies used for FACS analysis included: APC anti-CD3, PE anti-CD4, PE-Cy7 anti-CD45RO, BV711 anti-CD49a (integrin α4), APC-Fire 750 anti-integrin β7, BV421 anti-CCR9, and Percp-Cy5.5 anti-CCR7, BV605 anti-CCR2, PE anti-CRTH2, PE anti-CCR10, PE-Cy7 anti-CCR4, Percp-Cy5.5 anti-CXCR3, APC anti-CCR6, BV605 anti-CD4, PE-CF594 anti-CD25 (from BD). Vital dyes include: fixable viability eFluor® 506, eFluor® 660 and eFluor® 780 (all from eBioscience). Rh123 and elacridar were purchased from Sigma-Aldrich. All FACS data was acquired on LSRII or FACSCanto II instruments (BD), and analyzed using FlowJo 9 or FlowJo 10 software (TreeStar, Inc.). (We're probably missing a bunch).

FACS sorting

Cells stained with cell-surface antibodies, as above, were passed through 70 μm nylon filters, resuspended in PBS plus 1% serum, and sorted on a FACS AriaII machine (BD Biosciences). Sorted cells were collected in serum-coated tubes containing PBS plus 50% serum. Gates used to sort MDR1+/- T cells, based on Rh123 efflux, were set using background Rh123 efflux in elacridar-treated cells. For human T cell sorts, Peripheral blood mononuclear cells (PBMC) were isolated using Ficoll-Plaque PLUS (GE Healthcare) from 25 mL of enriched buffy coats (OneBlood). $CD4^+$ T cells were enriched using the Human total CD4 T cell Negative Isolation kit (EasySep), followed by enrichment of either effector/memory T cells (Human Memory CD4 T cell Enrichment kit; EasySep) or Treg cells (Human $CD4^+CD127^{lo}CD49d^-$ Treg Enrichment Kit; EasySep) (all from StemCell Technologies). Enriched cells were stained with anti-human FACS antibodies (listed above) for 20 minutes on ice. Stained cells were filtered through sterile 40 uM mesh filters and re-suspended in PBS with 5% FBS and 0.1% DNase. In cases where RNA was isolated after sorting, 100,000 cells were sorted into 200 uL PBS with 1 uM DTT

and 5 uL RNase Inhibitor Cocktail (Takara); for *ex vivo* culture experiments, 0.4-1.2 x10^6 cells were sorted into complete T cell media.

Pooled *in vivo* shRNAmir screen

Two independent pooled screens were performed. Briefly, PLAT-E cells were cultured in 96 well plates with 5 x 10^4 per well in 100uL complete medium and transfected as described above. Magnetically enriched $CD4^+CD25^-$ T cells from spleens of 7- to 8-week old female FVB/N (FVB) mice were activated with anti-CD3 and anti-CD28 in 96 well plates and transduced 24 hr post-activation. Transduction efficiency of each individual shRNA was determined on day 4; transduced cells were pooled and FACS-sorted for ametrine$^+$ on day 5 and adoptively transferred (i. p.) into 10 FVB.*Rag1*$^{-/-}$ mice. An aliquot of sorted cells was saved for genomic DNA isolation and used for input reference. Six weeks post-transfer, live (viability dye$^-$) transduced (ametrine$^+$) $Rh123^{hi}$ ($Mdr1^-$) or $Rh123^{lo}$ ($Mdr1^+$) effector/memory T cells (Teff; $CD4^+CD25^-CD62L^{lo}CD44^{hi}$) were FACS-sorted from the spleen or small intestine lamina propria of FVB.*Rag1*$^{-/-}$ recipients. High quality genomic DNA was isolated using PureLink® Genomic DNA Mini Kit (Invitrogen) and 100 ng of DNA was used for library preparation. gDNA derived from transduced and sorted T cells were quantified with Qubit DNA assay. 75ng of gDNA were used as template in duplicate reactions to add the Ion adapter sequences and barcodes. Based on previous data, 28 cycles of PCRs were used to amplify the libraries using primers with Ion P1 miR30 loop sequence (5'-CCTCTCTATGGGCAGTCGGTGATTACATCTGTGGCTTCACTA-3') and Ion A miR-30 (5'-CCATCTCATCCCTGCGTGTCTCCGACTCAGXXXXXXXXXXGCTCGAGAAGGTATATTGCT-3') sequences. The miR-30 loop (PI) and miR-30 (A) annealing sequences are underlined. The IonXpress 10 nt barcode is depicted with a string of X's. Sequencing libraries were purified with 1.6X Ampure XP beads (Beckman Coulter), quantified with Qubit DNA HS assay (Invitrogen), and visualized on the Agilent 2100 Bioanalyzer (Agilent Technologies, Inc.). Individually-barcoded libraries were pooled at equimolar ratios and templated on to Ion spheres at 50 pM loading concentration using the Ion Chef (Life Technologies) with the Ion PI IC 200 kit. The templated Ion spheres (ISPs) were quantified using AlexaFluor sequence-specific probes provided in the Ion Spehere quality control kit (Life Technologies). The percent templated ISPs within 10-20% were taken forward to loading on the Ion PI V2 chips and then run on the Ion Proton with 200 bp reads. Libraries were sequenced using the Ion Torrent technology from Life Technologies following the manufacturer's instructions. Sequencing reads were aligned to the reference library using BLAST with default settings and raw counts were normalized with DESeq2. Normalized reads of shRNAmirs displaying $\leq$ 10-fold change between input and *ex vivo* spleen samples were considered for downstream analysis. The relative enrichment or depletion of shRNAmirs from each

population was determined by median $\log_2$ fold-change in abundance of shRNAmirs in Mdr1^{hi} *vs*. Mdr1^{lo} siLP Teff cells.

Compounds and tissue extracts

10 or 20 uM 1,4-Bis-[2-(3,5-dichloropyridyloxy)]benzene, 3,3′,5,5′-Tetrachloro-1,4-bis(pyridyloxy) benzene (TC), 10 uM 5α-Androstan-3β-ol (And), 10 uM 5-Pregnen-3β-ol-20-one-16α-carbonitrile (PCN) (all from Sigma-Aldrich)—or serum, bile (from gallbladder), sterile soluble small intestine lumen content (siLC), or sterile soluble colon lumen content (cLC) from wild type (B6) mice—were added to mouse naïve or effector/memory (Teff) cells stimulated with anti-CD3/anti-CD28 antibodies as above. For preparation of mouse tissue extracts, mouse small intestinal lumen content (siLC) or colon lumen content (cLC) was extracted from whole tissue into a sterile tube. Contents were weighed, diluted with an equal volume of sterile PBS, vortexed vigorously for 30 sec, and then supernatants were collected after sequential centrifugation steps: (*i*) 10 min at 930 x *g*; and (*ii*) 10 min at 16 x *g*. Cleared supernatants were finally sterile-filtered using 0.22 μm filters and aliquots were frozen at -20^{o} C. Serum was collected in EDTA coated tubes and centrifuged for 5 min at 2.4 x *g*. Due to small sample size, serum and gallbladder bile were used directly without filter sterilization after harvesting. Equal volumes of sterile vehicles (DMSO for TC, And; ethanol for PCN; PBS for sterile mouse content) served as negative controls. For human T cell culture experiments, healthy adult donor PBMC were FACS-sorted for the following subsets: (*i*) naïve CD4$^+$ T cells (CD4$^+$CD25$^-$CD45RO$^-$CCR7^{hi}); (*ii*) Treg cells (CD4$^+$CD25^{hi}); (*iii*) α4$^-$CCR9$^-$ effector/memory cells (Teff; CD4$^+$CD25$^-$CD45RO$^+$); and (*iv*) α4$^+$CCR9$^+$ effector/memory cells (Teff; CD4$^+$CD25$^-$CD45RO$^+$). Note that all α4$^-$CCR9$^-$ Teff cells are integrin β7$^-$ and all α4$^+$CCR9$^+$ Teff cells are integrin β7$^+$. For all subsets, 30,000 purified cells were stimulated in round-bottom 96-well plates with human anti-CD3/anti-CD28 T cell expander beads (1 bead/cell; ThermoFisher) in complete media containing 10 U/mL rhIL-2 with or without 10 or 20 uM 6-(4-Chlorophenyl)imidazo[2,1-b][1,3]thiazole-5-carbaldehyde O-(3,4-dichlorobenzyl)oxime (CITCO) (Sigma-Aldrich); an equal volume of DMSO served as the negative control.

qPCR

RNA was isolated from cultured or ex vivo-isolated cells using RNeasy Mini columns with on-column DNase treatment (Qiagen); RNA was used to synthesize cDNA via a high capacity cDNA reverse transcription kit (Life Technologies). Taqman qPCR was performed on a StepOnePlus real time PCR instrument (Life Technologies/Applied Biosystems) using commercial Taqman primer/probe sets (Life

Technologies). Probes for mouse genes included: *Abcb1a* (Mm00607939_s1), *Nr1i3* (Mm01283981_g1), *Cyp2b10* (Mm01972453_s1), *Il10* (Mm01288386_m1) and *Actin b (Mm00607939_s1)*; probes for human genes included: *NR1I3* (Hs00901571_m1), *ABCB1* (Hs00184500_m1), *CYP2B6* (Hs04183483), *IL10* (Hs00961622_m1), and *ACTIN B* (Hs0160665_g1).

Bioinformatics analyses

ChIP-seq: Raw sequencing reads for CAR were downloaded from Gene Expression Omnibus (GSE112199)[17], aligned to USC mm10 with Bowtie2[33] and analyzed with MACS[34] using base settings. Biological replicate reads files were merged into a single file and bigwig files were generated and visualized with Integrated Genome Viewer (IGV)[35]. Peaks were filtered to remove reads with alternative annotations, mitochondrial DNA, or blacklist regions in R using GenomeInfoDb and GenomicRanges package.

RNA-seq: Next-generation RNA-sequencing (RNA-seq) was performed on FACS-sorted B6 wild type and CAR-deficient effector/memory T cells (Teff cells: viability dye^{-}CD45^{+}CD3^{+}CD4^{+}CD25^{-}CD44^{hi}) from spleen, small intestinal lamina propria, and colon lamina propria of *Rag1*$^{-/-}$ mice injected 3-weeks prior with congenic mixtures of CD45.1 wild type and CD45.2 *Nr1i3*$^{-/-}$ naïve T cells, approximately 500 sorted cells were processed directly to generate cDNA using the Clontech SMART-Seq v4 Ultra Low Input Kit (Clontech, Inc.) on three biologically-independent replicates. The generated cDNA was size selected using beads to enrich for fragments > 400 bp. The enriched cDNA was converted to Illumina-compatible libraries using the NEBNext Ultra II DNA kit (New England Biolabs, Inc.) using 1ng input. Final libraries were validated on the Agilent 2100 bioanalyzer DNA chips and quantified on the Qubit 2.0 fluorometer (Invitrogen, Life Technologies). Barcoded libraries were pooled at equimolar ratios and sequenced using single-end 75 bp reads on a NextSeq 500 instrument (Illumina). Raw sequencing reads (fastq files) were mapped to the mm10 transcriptome and transcript abundance in terms of Transcripts Per Million (TPM) were quantified using Salmon[48]. PCA was performed and projected in R-studio. Differentially expressed genes (DEG) were determined using DESeq2 ($P < .05$) for CAR-deficient (B6.*Nr1i3*$^{-/-}$) *vs.* wild type (B6) Teff cells from spleen (296 up; 285 down), siLP (472 up; 523 down), or cLP (350 up; 228 down) and $\log_2$ fold-change was used as the ranking metric to generate input ranked lists for gene set enrichment analysis (GSEA) (https://www.gsea-msigdb.org/gsea/index.jsp); these genes were compared against both customized and curated gene sets (the latter from the Molecular Signature Database (MSigDB)) for enrichment—quantified as normalized enrichment score (NES)—and visualized using ggplot2 package in R. Differentially expressed genes of wild type (B6) Teff cells from the spleen, siLP, or cLP determined by DESeq2 were used to generate tissue-specific Teff gene

sets: (*i*) up in B6 spleen Teff, genes selectively expressed in spleen *vs*. either siLP or cLP wild type (B6) Teff cells; (*ii*) up in B6 siLP Teff, genes selectively expressed in siLP *vs*. either spleen or cLP wild type (B6) Teff cells; and (*iii*) up in B6 cLP Teff, genes selectively expressed in cLP *vs*. either spleen or siLP wild type (B6) Teff cells. RNA-seq data of pharmacological activation of CAR or PXR in hepatocytes *in vivo* from mice treated with the CAR agonist, TCPOBOP (TC), the PXR agonist, PCN, or vehicle (corn oil) (GSE104734)[16] were analyzed to generate the gene sets: Up in Hep + TC, genes selectively induced by the CAR agonist, TCPOBOP (TC), compared with either vehicle (corn oil) or the PXR agonist, PCN, in hepatocytes from mice treated with compounds *in vivo*; and Up in Hep + PCN, genes selectively induced by the PXR agonist, PCN, compared with either vehicle (corn oil) or the CAR agonist, TC, in hepatocytes from mice treated with compounds *in vivo*. Differential gene expression of *in vitro*-differentiated Tr1 (GSE92940)[22] and Th17 cells (GSE21670)[36] were determined using the Limma package in R (for microarray data)[37] to generate the gene sets: Tr1-signature, genes selectively expressed in *in vitro*-differentiated Tr1 cells, compared with non-polarizing conditions; and Th17-signature, genes selectively expressed in *in vitro*-differentiated Th17 cells, compared with non-polarizing conditions. Th1-signature, Th2-signature, induced (i)Treg-signature (GSE14308)[38], or T follicular helper (Tfh)-signature (GSE21379)[39], genes selectively induced in these *vs*. other T cell subsets, as curated on MSigDB (https://www.gsea-msigdb.org/gsea/msigdb/index.jsp).

TR-FRET co-regulator recruitment assay

The DNA sequences encoding mouse (m)CAR ligand-binding domain (LBD; residues 109 – 358) were amplified by PCR reaction and inserted into modified pET24b vectors to produce pET24b-mCAR-LBD. pACYC-Duet1-RXR-LBD, an expression plasmid for untagged human (h)RXRα LBD was provided by Dr. Eric Xu[40]. Purification of the mCAR-hRXRα LBD heterodimer, as well as hRXRα homodimer, was achieved by nickel-affinity chromatography, followed by size-exclusion chromatography in an Akta explorer FPLC (GE Healthcare). Briefly, pET24b-mCAR-LBD and pACYC-Duet1-RXR-LBD were co-transformed into BL21 (DE3) for mCAR-hRXRα heterodimer and pET46-RXRα-LBD was transformed into BL21 (DE3) for RXRα homodimer. The cells were grown in 4 x 900 mL of LB media at 37 °C until the OD600 reached a value of 0.6–0.7. Overexpression was induced by 0.3 mM of IPTG and the cells were grown further for 22 hr at 18 °C. The harvested cells were resuspended in sonication buffer (500 mM NaCl, 10 mM HEPES, 10 mM imidazole, pH 8.0, and 10% glycerol), sonicated on an ice-water bath for 20 min at 18 W output, and centrifuged for 25 min at 50,000 x g. The proteins were isolated from the sonicated supernatant by applying to a 2 mL His Select column and eluted with linear gradient

from 10 mM to 300 mM imidazole in sonication buffer. The elution fractions containing the proteins concentrated while exchanging buffer to gel filtration buffer (300 mM NaCl, 20 mM HEPES, 1 mM DTT, 5 % glycerol). The proteins were purified further by gel filtrations through a Superdex 200 26/60 column (GE Healthcare) equilibrated with gel filtration buffer. Fractions containing the proteins were pooled and concentrated to ~ 8 mg/mL each with 30 kDa cutoff ultrafiltration units (Millipore). Time-resolved fluorescence resonance energy transfer (TR-FRET) assays were performed in low-volume black 384-well plates (Greiner) using 23 µL final well volume. Each well contained the following components in TR-FRET buffer (20 mM KH_2PO_4/K_2HPO_4, pH 8, 50 mM KCl, 5 mM TCEP, 0.005% Tween 20): 4 nM 6xHis-CAR/RXRα LBD heterodimer or 6xHis-RXRα/RXRα homodimer LBD, 1 nM LanthaScreen Elite Tb-anti-His Antibody (ThermoFisher #PV5895), and 400 nM FITC-labeled PGC1α peptide (residues 137–155, EAEEPSLLKKLLLAPANTQ, containing an N-terminal FITC label with a six-carbon linker, synthesized by Lifetein). Pure ligand (TC, 9-*cis* RA) or tissue extracts (see above) were prepared via serial dilution in vehicle (DMSO or PBS, respectively), and added to the wells along with vehicle control. Plates were incubated at 25 °C for 1 hr and fluorescence was measured using a BioTek Synergy Neo plate reader (Promega). The terbium (Tb) donor was excited at 340 nm, its emission was monitored at 495 nm, and emission of the FITC acceptor was monitored at 520 nm. Data were plotted as 520/340 nM rations using Prism software (GraphPad); TC data were fit to a sigmoidal dose response curve equation.

Quantification and Statistical Analyses

Statistical analyses were performed using Prism (GraphPad). *P* values were determined by paired or unpaired student's *t* tests, Log-rank test, one-way ANOVA, and two-way ANOVA analyses as appropriate and as listed throughout the Figure legends. Statistical significance of differences (* $P < 0.05$, ** $P < 0.01$, *** $P < 0.001$, **** $P < 0.0001$) are specified throughout the Figure legends. Unless otherwise noted in legends, data are shown as mean values ± S.E.M.

Data availability

RNA-seq data for wild type and CAR-deficient effector $CD4^+$ T cells from spleen, small intestine lamina propria or colon lamina propria of congenically co-transferred *Rag1*$^{-/-}$ mice, as well as from human peripheral blood $\alpha4^+\beta7^+CCR9^+$ memory $CD4^+$ T cells stimulated *ex vivo* in the presence or absence of the human CAR agonist, CITCO, are available on the NCBI Gene Expression Omnibus (GEO) repository (accession ID: GSE149220).

Figure legends

Fig. 1. A pooled *in vivo* RNAi screen identifies CAR as a transcriptional regulator of MDR1 expression in mucosal T cells. (a) Naïve CD4$^+$ T cells from spleens of wild type FVB/N mice (FVB Tnaive), were activated and transduced in 96-well plates with a library of 258 retroviruses expressing unique shRNAmirs against 70 genes together with the retroviral reporter, Ametrine (one shRNAmir clone per well; see supplementary online information for details of the screening library). Transduced cells were expanded until day 5, after which cells were pooled, FACS-sorted (as Ametrine$^+$ cells), and transferred as a pool into FVB.*Rag1*$^{-/-}$ recipients; an aliquot of the pooled and sorted "input" cells (*i.e.*, prior to *in vivo* transfer) was frozen for subsequent analysis. Viable transduced (Ametrine$^+$) effector/memory (Teff; CD4$^+$CD25$^-$CD62L^{lo}CD44^{hi}) cells were re-isolated by FACS-sorting 6-weeks post-T cell transfer from spleen or small intestine lamina propria (siLP). Total transduced spleen Teff cells were collected, and both spleen and siLP Teff cells were further sub-divided into Mdr1^{hi} and Mdr1^{lo} subsets, based on efflux of the Mdr1 fluorescent substrate, Rh123. gDNA from all 6 Teff cell pools were subjected to DNA-seq to quantify shRNAmir abundance. **(b)** Median $\log_2$ fold-change in abundance of shRNAmirs in Mdr1^{hi} *vs*. Mdr1^{lo} siLP Teff cells. Dashed horizontal lines indicate 2-fold changes. Data incorporates shRNAmir abundance, determined by DNA-seq, in 2-indpeendent screens using pooled spleens and siLP from 10 transferred FVB.*Rag1*$^{-/-}$ mice per screen. **(c)** Diagram of the *Nr1i3*/CAR locus. Seed sequence positions for each of the 5 shRNAmirs targeting CAR (*shNr1i3s*) are shown; 5' and 3' untranslated regions (UTR) are indicated; filled boxes depict exons. **(d)** Mean weight loss (± SEM) in co-housed FVB.*Rag1*$^{-/-}$ mice injected with FVB wild type CD4$^+$ T cells transduced *in vitro* with a negative control shRNAmir against CD8 (*shCd8a*; $n = 11$), or the indicated shRNAmirs against CAR (*shNr1i3*s); *shNr1i3.1* ($n = 7$), *shNr1i3.2* ($n = 7$), *shNr1i3.3* ($n = 7$), *shNr1i3.4* ($n = 7$), *shNr1i3.5* ($n = 7$). *** $P < .001$, **** $P < .0001$, Two-way ANOVA. **(e)** Correlation between mean weight loss induced by Teff cells in FVB.*Rag1*$^{-/-}$ recipients (at 6-weeks post-T cell transfer; as in [d]) and mean percent of Mdr1-dependent Rh123 efflux in *ex vivo*-isolated spleen Teff cells (determined by flow cytometry as in Extended Data Fig. 1c-d). ** $P < .01$, Pearson (r) correlation test. **(f)** Mean weight loss (± SEM) in B6.*Rag2*$^{-/-}$ mice transplanted with naïve CD4$^+$ T cells from spleens of C57BL/6 wild type (B6; blue; $n = 7$) or CAR-deficient (B6.*Nr1i3*$^{-/-}$; red; $n = 9$) mice. ** $P < .01$, Two-way ANOVA. **(g)** H&E-stained sections of colons or terminal ilea from co-housed B6.*Rag2*$^{-/-}$ mice 6-weeks after transfer of wild-type (B6) or CAR-deficient (B6.*Nr1i3*$^{-/-}$) naïve CD4$^+$ T cells as in (f). Representative of 7-9 mice per group from 2-independent experiments. **(h)** Mean histology scores (± SEM) for colons or terminal ilea from

co-housed B6.*Rag2*$^{-/-}$ mice injected with wild-type (B6; n =7) or CAR-deficient (B6.*Nr1i3*$^{-/-}$; n = 9) naïve CD4^{+} T cells as in (f-g). ** $P < .01$, two-tailed Mann-Whitney test.

Fig. 2. CAR reprograms T cell gene expression in the small intestine. (a) Equal numbers of CD45.1 wild type (B6; blue) and CD45.2 CAR-deficient (B6.*Nr1i3*$^{-/-}$; red) naïve CD4^{+} T cells were transferred together into B6.*Rag1*$^{-/-}$ mice. Resulting T effector (Teff) cells were FACS-purified 3-weeks later from spleen, small intestine lamina propria (siLP), or colon lamina propria (cLP) and transcriptional profiles were assessed by RNA-seq. **(b)** Principle component analysis (PCA) of gene expression in *ex vivo*-isolated wild type (B6) or CAR-deficient (B6.*Nr1i3*$^{-/-}$) Teff cells from spleen, siLP, or cLP of congenically co-transferred B6.*Rag1*$^{-/-}$ mice as in (a). **(c)** *Top*, overlap, presented as Venn diagrams, between genes expressed significantly higher in B6 wild type effector/memory (Teff) cells re-isolated from spleen, small intestine lamina propria (siLP) or colon lamina propria (cLP) of week 3 T cell-reconstituted B6.*Rag1*$^{-/-}$ mice (as in [a]), compared with each other. Genes expressed significantly higher in spleen-, siLP- or cLP-derived wild type Teff cells, compared with wild type counterparts from the other two tissues—referred to here as spleen, siLP or cLP Teff signature (sig) genes—were used for downstream analyses. *Bottom*, differential genes expression, determined by DEseq2 and presented as volcano plots, between wild type (B6) and CAR-deficient (B6.*Nr1i3*$^{-/-}$) Teff cells from the spleen, siLP or cLP of week 3 T cell-reconstituted B6.*Rag1*$^{-/-}$ mice (as in [a]). Numbers of differentially-expressed genes (Up; Down) are indicated in grey text for each comparison; examples of wild type siLP-signature genes showing reduced expression in CAR-deficient *vs*. wild type Teff cells are annotated in green text. **(d)** *Left*, gene set enrichment analysis (GSEA) showing that siLP B6 wild type Teff cell signature genes (siLP B6 Teff sig; determined as in [c]) are significantly enriched within those expressed lower in B6.*Nr1i3*$^{-/-}$ *vs*. wild type siLP Teff cells. Normalized enrichment score (NES) and P value is indicated. *Right*, GSEA summary plot showing enrichment of tissue-specific (spleen, siLP, cLP) wild type Teff cell signature genes (determined as in [c]; x-axis) within genes differentially expressed between CAR-deficient (B6.*Nr1i3*$^{-/-}$) and wild type (B6) Teff cells from spleen, siLP or cLP (y-axis). Circle sizes are proportional to -$\log_{10}$ adjusted P (Padj) values; color represents directionality of enrichment, based on NES. (b-d) Mean normalized gene expression values, expressed as TPM, are shown from 3-independent experiments using Teff cells purified from pooled tissues of 5 congenically co-transferred B6.*Rag1*$^{-/-}$ mice per experiment. **(e)** Mean relative expression ($\pm$ SEM; n = 3) of *Abcb1a* or *Cyp2b10*, determined by qPCR, in wild type (B6) or CAR-deficient (B6.*Nr1i3*$^{-/-}$) Teff cells re-isolated from spleens of congenically co-transferred B6.*Rag1*$^{-/-}$ mice (as in [a]) and stimulated *ex vivo* with anti-CD3/anti-CD28 antibodies in the presence or absence of tissue extracts isolated from wild type (B6) mice. Veh, vehicle;

644 TC, CAR agonist TCPOBOP; siLC, small intestine lumen content; bile, from gallbladder; cLC, colon
645 lumen content. * $P < .05$, ** $P < .01$, *** $P < .001$, One-way ANOVA with Dunett's correction for
646 multiple comparisons. NS, not significant. **(f)** Mean activation (± SEM; triplicate samples) of
647 recombinant mouse (m)CAR-human (h)RXRα ligand-binding domain (LBD) heterodimers, determined
648 by time-resolved fluorescence resonance energy transfer (TR-FRET), in the presence of the mCAR
649 agonist, TCPOBOP (TC; blue) or the hRXRα agonist, 9-*cis* retinoic acid (RA; red). Median effective
650 concentrations (EC_{50}'s) of TC-dependent bi-phasic mCAR:hRXRα LBD heterodimer activation are
651 indicated. Representative of more than 5-independent experiments. **(g)** Mean activation (± SEM; $n = 3$)
652 of mCAR:hRXRα LBD heterodimers, determined by TR-FRET as in (f), in the presence of titrating
653 concentrations of siLC, bile, cLC or serum from wild type B6 mice. The 4 bars for each tissue extract
654 are *(left to right)*: (1) diluent (PBS) alone; (2) 0.01%, (3) 0.1%, and (4) 1%. Data are shown from 3-
655 independent experiments using extracts from different wild type mice; each concentration from each
656 individual mouse was run in triplicate. * $P < .05$, **** $P < .0001$, one-way ANOVA with Tukey's
657 correction for multiple comparisons. NS, not significant.
658
659 **Fig. 3. CAR promotes *Il10* gene expression in T cells. (a)** Gene set enrichment analysis (GSEA)
660 showing enrichment of genes previously associated with type 1 regulatory (Tr1) cells[21] amongst those
661 expressed at lower levels in CAR-deficient (B6.*Nr1i3*$^{-/-}$) *vs*. wild type (B6) small intestine lamina propria
662 (siLP) Teff cells (as in Fig. 2a-d). Normalized enrichment score (NES) and *P* value are listed. **(b)** GSEA
663 summary plot showing enrichment of gene sets previously assigned to major effector and regulatory T
664 cell lineages (see methods for details) within genes differentially expressed between CAR-deficient
665 (B6.*Nr1i3*$^{-/-}$) and wild type (B6) Teff cells from spleen, siLP or cLP (y-axis). Circle sizes reflect -$\log_{10}$
666 adjusted *P* (Padj) values; color represents directionality of enrichment, based on NES. **(c)** *Ex vivo Il10*
667 gene expression, displayed as transcripts per million (TPM) and determined by RNA-seq ($n = 3$), in *ex*
668 *vivo*-isolated wild type (B6; blue) or CAR-deficient (B6.*Nr1i3*$^{-/-}$; red) Teff cells from spleen, siLP, or
669 cLP of congenically transferred B6.*Rag1*$^{-/-}$ mice (as in Fig. 2a). *P* values (paired two-tailed student's *t*
670 test) are indicated. **(d)** *Left*, equal numbers of CD45.1 CAR-sufficient (10BiT; blue) and CD45.2 CAR-
671 deficient (*Nr1i3*$^{-/-}$ 10BiT; red) *Il10*-Thy1.1 reporter naïve CD4^{+} T cells were transferred together into
672 B6.*Rag1*$^{-/-}$ mice. Expression of the *Il10* reporter (10BiT) allele in Teff cells from spleen, siLP, or cLP
673 was analyzed after 2 weeks by *ex vivo* flow cytometry analysis of Thy1.1 expression. *Right*, *Il10*
674 expression, identified by Thy1.1 staining, in CD45.1^{+} CAR-sufficient or CD45.1^{-} (CD45.2) CAR-
675 deficient Teff cells from spleen, siLP, or cLP of week 2 reconstituted *Rag1*$^{-/-}$ mice. Representative of 4

mice analyzed over 2-independent experiments. **(e)** Mean percentages (n = 4; ± SEM) of Thy1.1 (*Il10*)-expressing wild type (B6, blue) or CAR-deficient (B6.*Nr1i3*$^{-/-}$) spleen, siLP, or cLP Teff cells, determined by *ex vivo* flow cytometry as in (d). * $P < .05$, ** $P < .01$, One-way ANOVA with Tukey's correction for multiple comparisons. **(f)** Mean relative *Il10* expression (± SEM; n = 3), determined by qPCR, in wild type (B6) or CAR-deficient (B6.*Nr1i3*$^{-/-}$) Teff cells re-isolated from spleens of congenically co-transferred B6.*Rag1*$^{-/-}$ mice (as in Fig. 2a, 2e) and stimulated *ex vivo* with anti-CD3/anti-CD28 antibodies in the presence or absence of tissue extracts isolated from wild type (B6) mice. Veh, vehicle; TC, CAR agonist TCPOBOP; siLC, small intestine lumen content; bile, from gallbladder; cLC, colon lumen content. * $P < .05$, ** $P < .01$, *** $P < .001$, One-way ANOVA with Tukey's correction for multiple comparisons. NS, not significant. **(g)** Mean relative CAR/*Nr1i3* gene expression (± SEM; n = 2), determined by qPCR, in B6 wild type naïve CD4^{+} T cells cultured for 4 days in polarizing conditions to generate effector or regulatory T cell subsets. Tr1 conditions included cells activated and expanded in the presence of IL-27 alone, dexamethasone (Dex) alone, or both together. npTh17, non-pathogenic Th17 cells; pTh17, pathogenic Th17 cells. **(h)** IL-10 and IFNγ expression in CD45.1 wild type (B6) or CD45.2 CAR-deficient (B6.*Nr1i3*$^{-/-}$) T cells activated and expanded together for 4 days in media alone, IL-27 alone, dexamethasone (Dex) alone, or IL-27 plus Dex. Cytokine expression was analyzed by intracellular cytokine staining after restimulation with PMA and ionomycin (see methods); representative of 5 experiments. Numbers indicate percentages. **(i)** Mean percentages (n = 5; ± SEM) of IL-10-expressing wild type (B6) or CD45.2 CAR-deficient (B6.*Nr1i3*$^{-/-}$) T cells after 4-day co-culture as in (h). * $P < .05$, paired two-tailed student's t test.

Fig. 4. Pharmacologic CAR activation suppresses bile acid-induced experimental ileitis. (a) Mean relative expression (± SEM; n = 3) of *Abcb1a*, *Cyp2b10*, or *Il10*, determined by qPCR, in wild type (B6; blue) or CAR-deficient (B6.*Nr1i3*$^{-/-}$; red) Teff cells isolated from spleens of congenically co-transferred B6.*Rag1*$^{-/-}$ mice 72 hr after a single dose of either the CAR agonist, TCPOBOP (TC), or vehicle. Data are shown as relative expression in Teff cells from TC- *vs*. vehicle-treated mice; individual data points reflect 3-independent TC treatment experiments in which wild type or CAR-deficient Teff cells were isolated from a pool of 5 spleens isolated from identically treated animals. * $P < .05$, paired two-tail student's t test. **(b)** Mean weight loss (± SEM) of co-housed *Rag2*$^{-/-}$ mice transplanted with wild-type naïve T cells and maintained on a CA-supplemented diet with (red; n = 18) or without (blue; n = 16) TC treatment. CA-fed *Rag2*$^{-/-}$ mice not reconstituted with T cells (no T cells; grey; n =10), or *Rag2*$^{-/-}$ mice transplanted with wild type T cells and left on control chow diet treated with vehicle (black, n = 17) are

also shown. Weights are presented relative to the start of TC treatment (3-weeks post-T cell transfer). * $P < .05$, ** $P < .01$, Two-way ANOVA. **(c)** *Top,* H&E-stained sections of terminal ilea or colons from control or CA-fed *Rag2*$^{-/-}$ mice reconstituted with wild type T cells and treated +/- TC as in (b). Representative of 3-4 mice/group. *Bottom,* mean histology scores (± SEM) for colons (n = 3-4) or terminal ilea (n = 3) as in (c). * $P < .05$, one-way ANOVA with Tukey's correction for multiple comparisons. NS, not significant. **(d)** Model of CAR-dependent mucosal T cell regulation in the small intestine. Bile acids reabsorbed by enterocytes in the ileum expressing the Apical sodium-dependent bile acid transporter (Asbt) accumulate in the lamina propria, inducing stress and inflammation, which may increase CAR expression in mucosal Teff cells. Other (non-BA) metabolites in bile directly activate the CAR ligand-binding domain (LBD), leading to increased expression of at least two discrete, yet functionally synergistic gene sets, which serve to detoxify BAs (e.g., MDR1Abcb1a, cytochrome P450 enzymes [CYPs]), suppress inflammation via IL-10 and support small bowel immune homeostasis.

Extended Data Figure Legends

Extended Data Figure 1. Nuclear receptor-dependent regulation of effector T cell persistence and MDR1 expression *in vivo*. (a) *Top*, abundance of shRNAmirs in *ex vivo*-isolated spleen and *in vitro*-transduced (input) Teff cells. shRNAmirs with ≤ 1 normalized read in both *ex vivo* spleen and input Teff cell pools were considered 'poorly represented' (highlighted green). Well-represented shRNAmirs displaying ≤ 10-fold change between *ex vivo* spleen and input Teff cell pools (between blue lines) were considered for downstream analysis. *Bottom*, abundance of shRNAmirs, filtered for minimal effects on *in vivo* Teff cell persistence, in *ex vivo*-isolated Mdr1^{hi} (Rh123^{lo}) and Mdr1^{lo} (Rh123^{hi}) siLP Teff cells. **(b)** Log_2 fold-change in abundance (± SEM) of shRNAmirs against *Cd19* (n = 3), *Abcb1a* (n = 2), *Nr1i3* (n = 5), *Thra* (n = 6), and *Esrra* (n = 3) in FVB wild type Rh123^{lo} (MDR1^{hi}) *vs*. Rh123^{hi} (MDR1^{lo}) effector/memory T cells (Teff; sorted as in Fig. 1a) recovered from spleens or small intestine lamina propria (siLP) of transferred FVB.*Rag1*$^{-/-}$ mice. (a-b) Data incorporates shRNAmir abundance, determined by DNA-seq, in 2-indpeendent screens using pooled spleens and siLP from 10 transferred FVB.*Rag1*$^{-/-}$ mice per screen. **(c)** *Ex vivo* Rh123 efflux, determined by flow cytometry, in FVB wild type Teff cells expressing a control shRNAmir against CD8 (*shCD8a*) or 1 of 5-independent shRNAmirs against CAR (*shNr1i3*) isolated from spleens of transferred FVB.*Rag1*$^{-/-}$ mice 6-weeks post-transfer. Rh123 efflux in transduced (Ametrine pos.; blue) cells is overlaid with that in congenically-transferred untransduced (Ametrine neg.; red) Teff cells from the same mouse. Background Rh123 efflux in

untransduced Teff cells treated with the MDR1 inhibitor, elacridar, is shown in gray. Representative of 63 mice analyzed over 3-independent experiments. **(d)** Mean normalized *ex vivo* Rh123 efflux (± SEM) in FVB wild type spleen Teff cells expressing control (*shCd8a*; $n = 11$) or CAR-targeting (shNr1i3) shRNAmirs; *shNr1i3.1* ($n = 10$), *shNr1i3.2* ($n = 10$), *shNr1i3.3* ($n = 12$), *shNr1i3.4* ($n = 10$), *shNr1i3.5* ($n = 10$), determined by flow cytometry as in (c). Rh123 efflux was normalized to control *shCd8a*-expressing Teff cells after calculating the change (Δ) in Rh123 mean fluorescence intensity (MFI) between congenically-transferred transduced (ametrine pos.) *vs*. untransduced (ametrine neg.) Teff cells. * $P < .05$, **** $P < .0001$, One-way ANOVA with Dunnett's correction for multiple comparisons. **(e)** Mean relative *Abcb1a*, *Nr1i3*, and *Cyp2b10* expression (± SEM), determined by qPCR, in FVB spleen Teff cells FACS-sorted from FVB.*Rag1*$^{-/-}$ recipient mice expressing either a negative control shRNAmir against CD8 (*shCd8a*; $n = 8$), or the indicated shRNAmirs against CAR (*shNr1i3*s); *shNr1i3.1* ($n = 8$), *shNr1i3.2* ($n = 8$), *shNr1i3.3* ($n = 8$), *shNr1i3.4* ($n = 8$), *shNr1i3.5* ($n = 8$).* $P < .05$, ** $P < .01$, *** $P < .001$, **** $P < .0001$, One-way ANOVA with Tukey's correction for multiple comparisons. **(f)** Median $\log_2$ fold change in shRNAmir abundance between FVB wild type *ex vivo*-isolated spleen *vs*. *in vitro*-transduced (input) Teff cells. (a, d) shRNAmir abundance reflects the mean number of normalized reads, by DNA-seq, in the indicated Teff subsets obtained in 2-independent screens, each using cells transferred into 10 FVB.*Rag1*$^{-/-}$ mice. **(g)** *Ex vivo* Rh123 efflux, determined by flow cytometry, in CD45.1 wild type (B6; red) or CD45.2 CAR-deficient (B6.*Nr1i3*$^{-/-}$), PXR-deficient (B6.*Nr1i2*$^{-/-}$) or CAR/PXR double-deficient (B6.*Nr1i3*$^{-/-}$*Nr1i2*$^{-/-}$) effector/memory T cells (Teff; gated as in Extended Data Fig. 8a; blue) isolated from spleens of B6.*Rag1*$^{-/-}$ mice 6-weeks post-naïve T cell congenic co-transfer. Background Rh123 efflux in CD45.1 B6 Teff cells treated with the MDR1 inhibitor, elacridar, is shown in gray. Representative of a total of 22 mice analyzed over two-independent T cell transfer experiments. **(h)** Mean normalized Rh123 efflux (± SEM) in congenically-transferred CD45.1 wild type (B6; $n = 7$) or CD45.2 CAR-deficient (B6.*Nr1i3*$^{-/-}$; $n = 7$), PXR-deficient (B6.*Nr1i2*$^{-/-}$; $n = 7$) or CAR/PXR double-deficient (B6.*Nr1i3*$^{-/-}$*Nr1i2*$^{-/-}$; $n = 7$) spleen Teff cells, determined by flow cytometry as in (g). * $P < .05$, One-way ANOVA with Tukey's correction for multiple comparisons. **(i)** Mean relative *Abcb1a* expression (± SEM), determined by *ex vivo* qPCR, in CD45.1 wild type (B6; $n = 5$) or CD45.2 CAR-deficient (B6.*Nr1i3*$^{-/-}$; $n = 5$), PXR-deficient (B6.*Nr1i2*$^{-/-}$; $n = 4$) or CAR/PXR double-deficient (B6.*Nr1i3*$^{-/-}$*Nr1i2*$^{-/-}$; $n = 5$) spleen Teff cells (sorted as in Extended Data Fig. 8a) from spleens of congenically-transferred B6.*Rag1*$^{-/-}$ as in (a). * $P < .05$, One-way ANOVA with Tukey's correction for multiple comparisons.

Extended Data Figure 2. Inhibition of bile acid reabsorption rescues ileitis induced by CAR-deficient T cells in reconstituted *Rag*$^{-/-}$ mice. (a) Mean weight loss (±SEM) of co-housed B6.*Rag2*$^{-/-}$ mice transplanted with wild type (B6; blue; n = 15) or CAR-deficient (B6.*Nr1i3*$^{-/-}$; red; n = 13) naïve CD4^{+} T cells and treated with 2% (w:w) cholestyramine (CME) beginning at 3-weeks post-T cell transfer. NS, not significant. **(b)** *Top*, H&E-stained sections of colons or terminal ilea from B6.*Rag2*$^{-/-}$ mice reconstituted with wild type or CAR-deficient T cells and treated +/- CME as in (a). Representative of 12 mice/group. *Bottom*, mean histology scores (± SEM; n = 12) for colons or terminal ilea as in (a). NS, not significant. **(c)** Mean weight loss (±SEM) of co-housed B6.*Rag1*$^{-/-}$ mice with or without the Apical sodium-dependent bile acid transporter (Asbt; gene symbol *Slc10a2*) after transplantation with wild type (B6; blue) or CAR-deficient (B6.*Nr1i3*$^{-/-}$; red) naïve CD4^{+} T cells. **(d)** *Top*, H&E-stained sections of terminal ilea or colons from control or Asbt-deficient B6.*Rag1*$^{-/-}$ mice reconstituted with wild type or CAR-deficient T cells as in (c). Representative of 5 mice/group. *Bottom*, mean histology scores (± SEM; n = 5) for colons or terminal ilea as above. * $P < .05$, ** $P < .01$, *** $P < .001$, One-way ANOVA with Tukey's correction for multiple comparisons. NS, not significant.

Extended Data Figure 3. Shared features of CAR-dependent gene expression in mucosal T cells and hepatocytes. (a) Overlap, presented as Venn diagrams, between genes induced in B6 wild type mouse hepatocytes by *in vivo* treatment with either the mouse CAR agonist, TCPOBOP (TC) or the mouse PXR agonist, PCN, relative to vehicle (CO, corn oil). **(b)** Summary gene set enrichment analysis (GSEA) plot showing that genes induced by TC, but not PCN, treatment in mouse hepatocytes (as in [a]), are enriched within those expressed at lower levels in CAR-deficient (B6.*Nr1i3*$^{-/-}$) *vs*. wild type (B6) siLP Teff cells from week-3 congenically co-transferred *Rag1*$^{-/-}$ mice (as in Fig. 2a-c). Normalized enrichment scores (NES) and *P* values are indicated by circle color and size, respectively. **(c)** Differential gene expression, determined by DEseq2 and shown as a volcano plot, between CAR-deficient (B6.*Nr1i3*$^{-/-}$) and wild type (B6) siLP Teff cells re-isolated from transferred B6.*Rag1*$^{-/-}$ mice, as in Fig. 2a. Genes induced by TC, but not PCN, treatment in mouse hepatocytes (as in [a]; purple), bound by CAR in ChIP-seq analysis of hepatocytes from TC-treated mice (blue), or both (red) are highlighted. Chi-square *P* values are indicated. **(d)** CAR-occupancy, determined by ChIP-seq, at representative loci whose expression is regulated by CAR in both mucosal T cells and hepatocytes within mouse hepatocytes ectopically expressing epitope-tagged mouse (m) or human (h) CAR proteins and re-isolated from mice after treatment with the mCAR agonist, TCPOBOP (TC), or the hCAR agonist, CITCO. * $P < 0.00001$; significant binding peaks were called in MACS using base settings.

Extended Data Figure 4. CAR promotes effector T cell persistence in the presence of small intestinal bile acids. **(a)** Percentages of live CD44^{hi} wild type (B6; CD45.1^{+}; blue) or CAR-deficient (B6.*Nr1i3*$^{-/-}$; CD45.1^{-}; red) effector/memory (Teff) cells, determined by flow cytometry and gated as in Extended Data Fig. 8a, in tissues of reconstituted B6.*Rag1*$^{-/-}$ mice over time. Numbers indicate percentages; representative of 5 mice per tissue and timepoint. **(b)** Fitness, defined as mean $\log_2$ fold-change (F.C.) of CAR-deficient (B6.*Nr1i3*$^{-/-}$) *vs*. wild type (B6) Teff cell percentages ($\pm$ SEM; $n = 5$) in tissues of congenically co-transferred *Rag1*$^{-/-}$ mice over time, determined by flow cytometry as in (a). **(c)** Percentage of wild type (B6, CD45.1^{+}; blue) and CAR-deficient (B6.*Nr1i3*$^{-/-}$, CD45.1^{-}; red) naïve (CD62L^{hi}) CD4^{+} T cells after sorting and mixing, and prior to *in vivo* transfer into *Rag1*$^{-/-}$ mice (input Tnaive); representative of 3 mixtures used for analyzing resulting Teff cells at 2- 4- or 6-weeks post-transfer. **(d)** Equal numbers of CD45.1 wild type (B6; blue) and CD45.2 CAR-deficient (B6.*Nr1i3*$^{-/-}$; red) naïve CD4^{+} T cells were transferred together into co-housed *Rag1*$^{-/-}$ mice with or without the ileal bile acid reuptake transporter, Asbt (gene symbol *Slc10a2*). Resulting effector (Teff) cells from small intestine lamina propria (siLP) were analyzed 2-weeks post- T cell transfer via flow cytometry. **(e)** Percentages of live CD44^{hi} wild type (B6; CD45.1^{+}; blue) or CAR-deficient (B6.*Nr1i3*$^{-/-}$; CD45.1^{-}; red) effector/memory (Teff) cells, determined by flow cytometry and gated as in Extended Data Fig. 8a, in siLP of week-2 reconstituted B6.*Rag1*$^{-/-}$ mice. Numbers indicate percentages; representative of 8-10 mice analyzed over two-independent experiments. **(f)** Mean absolute numbers ($\pm$ SEM) of live CD45.1 wild type (B6; *left*) or CD45.2 CAR-deficient (B6.*Nr1i3*$^{-/-}$; *right*) Teff cells, determined by *ex vivo* flow cytometry as in (e), from siLP 2-weeks after mixed T cell transfer into control (Asbt$^{+/+}$; blue; $n = 8$) or Asbt-deficient (Asbt$^{-/-}$; red; $n = 10$) *Rag1*$^{-/-}$ recipients. Fold-changes in cell numbers recovered from Asbt-deficient *vs*. control recipients, as well as *P* values (two-tailed unpaired student's t test) are indicated.

Extended Data Figure 5. Preferential CAR expression and function in human effector/memory T cells expressing small bowel homing receptors. (a) FACS-based identification of human CD4^{+} T cell subsets in PBMC from healthy adult human donors. Expression of integrin α4 (α4 int.) in gated naïve (gray), T regulatory (Treg; blue), or effector/memory (Teff; red) T cells is shown at right. **(b)** Expression of integrin β7 (β7 int.) and CCR9 in total naïve CD4^{+} T cells, or in α4 int.+/- Treg or Teff subsets (gated as in (a)). Representative of 13-independent experiments using PBMC from different donors. **(c)** Percentages (%) of α4^{+}β7^{+}CCR9^{+} Tnaive, Treg, or Teff cells, determined by flow cytometry as in (a-b). Individual data points for the 13 independent experiments are shown and connected by grey lines. ** *P*

< .01, One-way ANOVA with Holm-Sidak's correction for multiple comparisons. **(d)** *Ex vivo* Rh123 efflux in $CD4^+$ T cell subsets (gated as in a-b) in the presence (gray) or absence (red) of the selective MDR1 inhibitor, elacridar. Representative of 8 experiments. **(e)** Mean percentages (± SEM; $n = 7$) of $Rh123^{lo}$ ($MDR1^+$) Teff subsets, determined by flow cytometry as in (d). * $P < .05$, ** $P < .01$, *** $P < .001$, One-way ANOVA with Tukey's correction for multiple comparisons. **(f)** Mean (± SEM) *ex vivo* expression, determined by qPCR, of CAR/*NR1I3* ($n = 12$), MDR1/*ABCB1* ($n = 12$) or *CYP2B6* ($n = 10$) in $\alpha4^-\beta7^-CCR9^-$ or $\alpha4^+\beta7^+CCR9^+$ Tnaive, Treg or Teff cells, FACS-sorted as in (a-b). (e-f) * $P < .05$, ** $P < .01$, One-way ANOVA with Tukey's correction for multiple comparisons. **(g)** Mean relative *CYP2B6* expression (± SEM; $n = 5$), determined by qPCR, in $CD4^+$ T cell subsets (as in (f)) activated *ex vivo* with anti-CD3/anti-CD28 antibodies in the presence or absence of titrating concentrations of the human CAR agonist, CITCO. Gene expression was analyzed 24 hr post-activation. *** $P < .001$, Two-way ANOVA. **(h)** Mean normalized MDR1/*ABCB1* or *CYP2B6* expression (± SEM), determined by RNA-seq and presented as transcripts per million (TPM), in FACS-sorted $\alpha4^+\beta7^+CCR9^+$ Teff cells stimulated *in vitro* (anti-CD3/anti-CD28) for 24 hr in the presence or absence of CITCO. Data from 4 replicate RNA-seq experiments are shown; ** $P < .001$, paired two-tailed student's *t* test. **(i)** Identification of $CD4^+$ naive (Tnaive; $CD25^-CD45RO^-$; grey) or effector/memory (Teff; $CD25^-CD45RO^+$; red) cells, by flow cytometry, from healthy adult human PBMC. For improved purity of Th1, Th2, Th17 and Th17.1 cells, CCR10-expressing Th22 cells were excluded. CCR6 expression in Tnaive (grey) or non-Th22 Teff cells (red) is shown at right; $CCR6^+$ or $CCR6^-$ Teff cells were gated to enrich for Th17 or non-Th17 lineages, respectively. **(j)** Expression of CCR4 and CXCR3 in $CCR6^-$ (non-Th17; *left*) or $CCR6^+$ (Th17; *right*) Teff cells identifies enriched $CCR6^-CCR4^{lo}CXCR3^{hi}$ (Th1; orange), $CCR6^-CCR4^{hi}CXCR3^{lo}$ (Th2; blue), $CCR6^+CCR4^{hi}CXCR3^{lo}$ (Th17; green), and $CCR6^+CCR4^{lo}CXCR3^{hi}$ (Th17.1; red) subsets. **(k)** Expression of integrin α4 (α4 int.; *top*) in Th2, Th1, Th17 and Th17.1 human Teff cells gated as in (a-b). Expression of integrin β7 (β7 int.) and CCR9 within α4 int^- (*middle*) or α4 int^+ (*bottom*) Th2, Th1, Th17 or Th17.1 cells gated as above. (a-c) Representative of 9-independent experiments using PBMC from different healthy adult donors. **(l)** Percentages ($n = 9$) of $\alpha4^+\beta7^+CCR9^+$ cells within *ex vivo* Th1, Th2, Th17, or Th17.1 Teff cells gated as in (a-c). Data from independent donors are connected by red lines. **(m)** MDR1-dependent Rh123 efflux in the indicated Th1, Th2, Th17, or Th17.1 Teff subsets gated based on expression of α4 int., β7 int., and/or CCR9 in the presence (grey) or absence (red) of elacridar. Representative of 8 independent experiments using PBMC from different donors. **(n)** Mean percentages (± SEM; $n = 8$) of $Rh123^{lo}$ ($MDR1^+$) cells within Th1, Th2, Th17, or Th17.1 Teff subsets gated based on expression of α4 int., β7 int., and/or CCR9 as in (e). * $P < .05$, ** P

869 < .01, *** P < .001, One-way ANOVA with Tukey's correction for multiple comparisons. ND, not
870 detectable; NS, not significant.
871
872 **Extended Data Figure 6. TCPOBOP promotes CAR-dependent gene expression in *ex vivo*-isolated**
873 **effector T cells. (a)** *Top left,* equal numbers of CD45.1 wild type (B6; blue) and CD45.2 CAR-deficient
874 (B6.*Nr1i3*$^{-/-}$; red) naïve CD4^{+} T cells were transferred together into B6.*Rag1*$^{-/-}$ mice. Resulting effector
875 (Teff) cells were FACS-purified from spleen after 3 weeks. *Right*, sequential gating strategy for re-
876 isolating wild type and CD45.2 CAR-deficient spleen Teff cells is shown. *Bottom left*, mean relative
877 *Abcb1a*, *Cyp2b10*, or *Il10* expression (± SEM; n = 4), determined by qPCR, in *ex vivo*-isolated wild type
878 (B6) or CAR-deficient (B6.*Nr1i3*$^{-/-}$) spleen Teff cells. These cells were used for *ex vivo* cell culture
879 experiments in the presence or absence of small molecule ligands ([b-c] below). * P < .05, ** P < .01,
880 paired two-tailed student's t test. **(b)** Mean relative expression (± SEM) of *Abcb1a* (n = 4), *Cyp2b10* (n
881 = 4), or *Il10* (n = 3), determined by qPCR, in wild type (B6) or CAR-deficient (B6.*Nr1i3*$^{-/-}$) Teff cells
882 isolated from transferred *Rag1*$^{-/-}$ mice (as in [a]), and stimulated *ex vivo* with anti-CD3/anti-CD28
883 antibodies (for 24 hr) in the presence or absence of the mouse (m)CAR agonist, TCPOBOP (TC; 10
884 μM), the mCAR inverse agonist, 5α-Androstan-3β-ol (And; 10 μM), or both. ** P < .01, *** P < .001,
885 **** P < .0001, one-way ANOVA with Tukey's correction for multiple comparisons. **(c)** Mean relative
886 *Abcb1a*, *Cyp2b10*, or *Il10* expression (± SEM; n = 5), determined by qPCR, in wild type (B6) or CAR-
887 deficient (B6.*Nr1i3*$^{-/-}$) Teff cells isolated and stimulated as in (a-b) in the presence or absence of TC (10
888 μM) or the mouse PXR agonist, PCN (10 μM). Data are presented as fold-change in mRNA abundance
889 relative to vehicle-treated cells (DMSO for TC; ethanol for PCN). **** P < .0001, one-way ANOVA
890 with Dunnett's correction for multiple comparisons. NS, not significant.
891
892 **Extended Data Figure 7. Characteristics of endogenous intestinal metabolites that activate the**
893 **CAR ligand-binding domain. (a)** Mean activation (± SEM; triplicate samples) of recombinant human
894 (h)RXRα ligand-binding domain (LBD) homodimers, determined by time-resolved fluorescence
895 resonance energy transfer (TR-FRET), in the presence of the mCAR agonist, TCPOBOP (TC; blue) or
896 the hRXRα agonist, 9-*cis* retinoic acid (RA; red). Median effective concentration (EC_{50}) of 9-*cis* RA-
897 dependent hRXRα LBD homodimer activation is indicated. Representative of more than 5-independent
898 experiments. **(b)** Mean activation (± SEM; n = 3) of hRXRα LBD homodimers, determined by TR-
899 FRET as in (a), in the presence of titrating concentrations of siLC, bile, cLC or serum from wild type B6
900 mice. * P < .05, **** P < .0001, one-way ANOVA with Tukey's correction for multiple comparisons.

NS, not significant. **(c)** Mean activation (± SEM; $n = 3$) of CAR:RXR LBD heterodimers, determined by TR-FRET, in the presence of titrating concentrations of siLC isolated from conventionally-housed (Conv) or germ-free (GF) wild type B6 mice pre-treated with or without cholestyramine (CME) to deplete free bile acids. *** $P < .001$, **** $P < .0001$, One-way ANOVA with Dunnett's correction for multiple comparisons. (a-c) The bars for each tissue extract indicate dilution series *(left to right)*: (1) diluent (PBS) alone; (2) 0.01%, (3) 0.1%, and (4) 1%. Data are shown from 3-independent experiments using extracts from different wild type mice, with each concentration from each individual mouse run in triplicate. **(d)** Mean TR-FRET signals (± SEM; $n = 3$) of CAR:RXR LBD heterodimers in the presence of titrating concentrations of individual bile acid (BA) species. NS, not significant, one-way ANOVA with Dunnett's correction for multiple comparisons. The bars for BAs indicate concentrations *(left to right)*: (1) vehicle (DMSO); (2) 10 μM; (3) 100 μM; and (4) 1000 μM. Data are shown from 3-independent experiments, where each BA concentration was run in triplicate.

Extended Data Figure 8. CAR is required for a transient wave of IL-10 production by mucosal T cells early after naïve T cell transfer into *Rag*$^{-/-}$ mice. **(a)** Equal numbers of CD45.1 wild type (B6; blue) and CD45.2 CAR-deficient (B6.*Nr1i3*$^{-/-}$; red) naïve CD4$^+$ T cells were transferred together into *Rag1*$^{-/-}$ mice. Resulting effector (Teff) cells were analyzed—using surface and intracellular flow cytometry after *ex vivo*-stimulation with phorbol myristate acetate (PMA) and ionomycin—at 2- 4- and 6-weeks from spleen, mesenteric lymph node (MLN), small intestine lamina propria (siLP), or colon lamina propria (cLP). Gating hierarchy is shown from a representative sample of MLN mononuclear cells at 2-weeks post-T cell transfer. **(b)** Intracellular IL-10 and IFNγ expression, determined by flow cytometry, in wild type (B6, blue; *left*) or CAR-deficient (B6.*Nr1i3*$^{-/-}$, red; *right*) non-Th17 Teff cells, gated as in (a), from tissues of T cell-reconstituted B6.*Rag1*$^{-/-}$ mice over time. Numbers indicate percentages; representative of 5 mice per tissue and time point. Mean percentages **(c)** or numbers **(d)** (± SEM; $n = 5$) of IL-10-expressing wild type (B6, *left*) or CAR-deficient (B6.*Nr1i3*$^{-/-}$, *right*) Teff cells, determined by *ex vivo* flow cytometry as in (a-b), from tissues of transferred B6.*Rag1*$^{-/-}$ mice over time. **(e)** Specificity of IL-10 intracellular staining, as validated by analysis of IL-10 production by CD45.1 wild type (B6; blue) or CD45.2 *Il10*$^{-/-}$ (red) Teff cells isolated from spleen or siLP of congenically co-transferred *Rag1*$^{-/-}$ mice. Representative of 6 mice analyzed over 2-independent experiments. **(f)** Percentages of CD3$^+$CD4$^+$ T cells in tissues of *Rag1*$^{-/-}$ mice transplanted with congenic mixtures of wild type and CAR-deficient naïve CD4$^+$ T cells over time, determined by flow cytometry as in Extended Data Fig. 11a. Representative of 5 mice per tissue and time point. **(g)** Mean absolute numbers of

$CD3^+CD4^+$ T helper (T_H) cells (± SEM; n = 5) in tissues of transferred B6.*Rag1*$^{-/-}$ mice over time, determined by flow cytometry as in (a). **(h)** Mean relative *ex vivo* CAR (*Nr1i3*), MDR1 (*Abcb1a*), *Cyp2b10*, or *Il10* gene expression (± SEM; n = 3), determined by qPCR, in wild type (B6) $CD4^+$ effector/memory (Teff) cells (sorted as in Extended Data Fig. 9a) from spleens of transferred B6.*Rag1*$^{-/-}$ mice over time.

Extended Data Figure 9. CAR is required for anti-CD3-induced IL-10 expression in mucosal effector and regulatory T cell subsets and suppresses Th17 cell accumulation in the *Rag*$^{-/-}$ transfer model. (a) *Top row*, expression of Foxp3 and RORγt, determined by intracellular staining after *ex vivo* (PMA+ionomycin) stimulation, in $CD4^+CD44^{hi}$ cells from spleen (*left*) or small intestine lamina propria (siLP, *right*) of wild type (B6, blue) or CAR-deficient (B6.*Nr1i3*$^{-/-}$, red) mice injected with or without isotype control (IgG) or anti-CD3 antibody. *Bottom 4 rows*, expression of IL-10 and IL-17A in wild type or CAR-deficient spleen or siLP T cell subsets from mice treated +/- isotype control (IgG) or anti-CD3 antibodies. Cells were gated and analyzed by flow cytometry as above. Numbers indicate percentages; representative of 3 mice per group and genotype analyzed over 2-independent experiments. **(b-c)** Mean percentages of IL-10-expressing T cell subsets (± SEM; n = 3), gated and analyzed by *ex vivo* flow cytometry as in (a), in spleen **(b)** or siLP **(c)** T_H cell subsets from wild type (B6, blue) or CAR-deficient (B6.*Nr1i3*$^{-/-}$, red) mice injected with or without isotype control (IgG) or anti-CD3 antibody. * $P < .05$, one-unpaired student's t test; some P values are listed directly. **(d)** Expression of RORγt and IL-17A, determined by intracellular FACS analysis as in Extended Data Figure 8a, in wild type (B6) or CAR-deficient (B6.*Nr1i3*$^{-/-}$) $CD4^+$ effector/memory (Teff) cells from tissues of reconstituted *Rag1*$^{-/-}$ mice 2-weeks post-mixed T cell transfer. Numbers indicate percentages; representative of 5 mice per tissue and time point. **(e)** Mean percentages of (± SEM; n = 5) of wild type (B6; blue) or CAR-deficient (B6.*Nr1i3*$^{-/-}$; red) $ROR\gamma t^+IL\text{-}17A^-$ Teff cells, determined by intracellular flow cytometry as in (a). * $P < .05$, paired two-tailed student's t test. **(f)** Expression of RORγt and IL-17A, determined by intracellular FACS analysis, in wild type (B6) or *Il10*$^{-/-}$ Teff cells from tissues of reconstituted *Rag1*$^{-/-}$ mice 2-weeks post-mixed T cell transfer. Numbers indicate percentages; representative of 5 mice per tissue and time point. **(g)** Mean percentages of (± SEM; n = 7) of wild type (B6; blue) or *Il10*$^{-/-}$ (red) $ROR\gamma t^+IL\text{-}17A^-$ Teff cells, determined by intracellular flow cytometry as in (c). * $P < .05$, ** $P < .01$, paired two-tailed student's t test. MLN, mesenteric lymph nodes; siLP, small intestine lamina propria; cLP, colon lamina propria.

Extended Data Figure 10. TCPOBOP protection against bile acid-induced ileitis requires CAR expression in T cells. (a) Mean weight loss (± SEM; n = 5/group) of co-housed B6.*Rag2*$^{-/-}$ mice transplanted with CAR-deficient (B6.*Nr1i3*$^{-/-}$) CD4^{+} naïve T cells and maintained on a CA-supplemented diet with or without TC treatment. Weights are shown relative to 3-weeks post-transfer when TC treatments were initiated. NS, not significant; two-way ANOVA. **(b)** H&E-stained sections of terminal ilea or colons from B6.*Rag2*$^{-/-}$ mice reconstituted with CAR-deficient T cells and treated as above and as indicated. Representative of 5 mice/group. **(c)** Mean histology scores (± SEM) for colons or terminal ilea as in (b). NS, not significant; paired student's t test.

References

1 Hofmann, A. F. & Hagey, L. R. Key discoveries in bile acid chemistry and biology and their clinical applications: history of the last eight decades. *Journal of lipid research* **55**, 1553-1595, doi:10.1194/jlr.R049437 (2014).

2 Poupon, R., Chazouilleres, O. & Poupon, R. E. Chronic cholestatic diseases. *J Hepatol* **32**, 129-140 (2000).

3 Arab, J. P., Karpen, S. J., Dawson, P. A., Arrese, M. & Trauner, M. Bile acids and nonalcoholic fatty liver disease: Molecular insights and therapeutic perspectives. *Hepatology* **65**, 350-362, doi:10.1002/hep.28709 (2017).

4 Cao, W. *et al.* The Xenobiotic Transporter Mdr1 Enforces T Cell Homeostasis in the Presence of Intestinal Bile Acids. *Immunity* **47**, 1182-1196 e1110, doi:10.1016/j.immuni.2017.11.012 (2017).

5 Lazar, M. A. Maturing of the nuclear receptor family. *J Clin Invest* **127**, 1123-1125, doi:10.1172/JCI92949 (2017).

6 Ludescher, C. *et al.* Detection of activity of P-glycoprotein in human tumour samples using rhodamine 123. *British journal of haematology* **82**, 161-168 (1992).

7 Pols, T. W., Noriega, L. G., Nomura, M., Auwerx, J. & Schoonjans, K. The bile acid membrane receptor TGR5 as an emerging target in metabolism and inflammation. *J Hepatol* **54**, 1263-1272, doi:10.1016/j.jhep.2010.12.004 (2011).

8 Zhang, J., Huang, W., Qatanani, M., Evans, R. M. & Moore, D. D. The constitutive androstane receptor and pregnane X receptor function coordinately to prevent bile acid-induced hepatotoxicity. *J Biol Chem* **279**, 49517-49522, doi:10.1074/jbc.M409041200 (2004).

9 Cerveny, L. *et al.* Valproic acid induces CYP3A4 and MDR1 gene expression by activation of constitutive androstane receptor and pregnane X receptor pathways. *Drug Metab Dispos* **35**, 1032-1041, doi:10.1124/dmd.106.014456 (2007).

10 Wei, P., Zhang, J., Egan-Hafley, M., Liang, S. & Moore, D. D. The nuclear receptor CAR mediates specific xenobiotic induction of drug metabolism. *Nature* **407**, 920-923, doi:10.1038/35038112 (2000).

11 Evans, R. M. & Mangelsdorf, D. J. Nuclear Receptors, RXR, and the Big Bang. *Cell* **157**, 255-266, doi:10.1016/j.cell.2014.03.012 (2014).

12 Staudinger, J. L. *et al.* The nuclear receptor PXR is a lithocholic acid sensor that protects against liver toxicity. *Proc Natl Acad Sci U S A* **98**, 3369-3374, doi:10.1073/pnas.051551698 (2001).

13 Ostanin, D. V. *et al.* T cell transfer model of chronic colitis: concepts, considerations, and tricks of the trade. *American journal of physiology. Gastrointestinal and liver physiology* **296**, G135-146, doi:10.1152/ajpgi.90462.2008 (2009).

14 Arnold, M. A. *et al.* Colesevelam and Colestipol: Novel Medication Resins in the Gastrointestinal Tract. *The American journal of surgical pathology*, doi:10.1097/PAS.0000000000000260 (2014).

15 Dawson, P. A., Lan, T. & Rao, A. Bile acid transporters. *Journal of lipid research* **50**, 2340-2357, doi:10.1194/jlr.R900012-JLR200 (2009).

16 Cui, J. Y. & Klaassen, C. D. RNA-Seq reveals common and unique PXR- and CAR-target gene signatures in the mouse liver transcriptome. *Biochim Biophys Acta* **1859**, 1198-1217, doi:10.1016/j.bbagrm.2016.04.010 (2016).

17 Niu, B. *et al.* In vivo genome-wide binding interactions of mouse and human constitutive androstane receptors reveal novel gene targets. *Nucleic Acids Res* **46**, 8385-8403, doi:10.1093/nar/gky692 (2018).

18 De Calisto, J. *et al.* T-cell homing to the gut mucosa: general concepts and methodological considerations. *Methods Mol Biol* **757**, 411-434, doi:10.1007/978-1-61779-166-6_24 (2012).

19 Maglich, J. M. *et al.* Identification of a novel human constitutive androstane receptor (CAR) agonist and its use in the identification of CAR target genes. *J Biol Chem* **278**, 17277-17283, doi:10.1074/jbc.M300138200 (2003).

20 Ramesh, R. *et al.* Pro-inflammatory human Th17 cells selectively express P-glycoprotein and are refractory to glucocorticoids. *J Exp Med* **211**, 89-104, doi:10.1084/jem.20130301 (2014).

21 Moore, L. B. *et al.* Pregnane X receptor (PXR), constitutive androstane receptor (CAR), and benzoate X receptor (BXR) define three pharmacologically distinct classes of nuclear receptors. *Mol Endocrinol* **16**, 977-986, doi:10.1210/mend.16.5.0828 (2002).

22 Karwacz, K. *et al.* Critical role of IRF1 and BATF in forming chromatin landscape during type 1 regulatory cell differentiation. *Nat Immunol* **18**, 412-421, doi:10.1038/ni.3683 (2017).

23 Gagliani, N. *et al.* Coexpression of CD49b and LAG-3 identifies human and mouse T regulatory type 1 cells. *Nat Med* **19**, 739-746, doi:10.1038/nm.3179 (2013).

24 Maynard, C. L. *et al.* Regulatory T cells expressing interleukin 10 develop from Foxp3+ and Foxp3- precursor cells in the absence of interleukin 10. *Nat Immunol* **8**, 931-941, doi:10.1038/ni1504 (2007).

25 Barrat, F. J. *et al.* In vitro generation of interleukin 10-producing regulatory CD4(+) T cells is induced by immunosuppressive drugs and inhibited by T helper type 1 (Th1)- and Th2-inducing cytokines. *J Exp Med* **195**, 603-616, doi:10.1084/jem.20011629 (2002).

26 Korn, T., Bettelli, E., Oukka, M. & Kuchroo, V. K. IL-17 and Th17 Cells. *Annu Rev Immunol* **27**, 485-517, doi:10.1146/annurev.immunol.021908.132710 (2009).

27 Sano, T. *et al.* An IL-23R/IL-22 Circuit Regulates Epithelial Serum Amyloid A to Promote Local Effector Th17 Responses. *Cell* **163**, 381-393, doi:10.1016/j.cell.2015.08.061 (2015).

28 Wan, Q. *et al.* Cytokine signals through PI-3 kinase pathway modulate Th17 cytokine production by CCR6+ human memory T cells. *J Exp Med* **208**, 1875-1887, doi:10.1084/jem.20102516 (2011).

29 Campbell, C. *et al.* Bacterial metabolism of bile acids promotes generation of peripheral regulatory T cells. *Nature* **581**, 475-479, doi:10.1038/s41586-020-2193-0 (2020).

30 Song, X. *et al.* Microbial bile acid metabolites modulate gut RORgamma(+) regulatory T cell homeostasis. *Nature* **577**, 410-415, doi:10.1038/s41586-019-1865-0 (2020).

31 Kim, J. J., Shajib, M. S., Manocha, M. M. & Khan, W. I. Investigating intestinal inflammation in DSS-induced model of IBD. *J Vis Exp*, doi:10.3791/3678 (2012).

32 Berg, D. J. *et al.* Enterocolitis and colon cancer in interleukin-10-deficient mice are associated with aberrant cytokine production and CD4(+) TH1-like responses. *J Clin Invest* **98**, 1010-1020, doi:10.1172/JCI118861 (1996).

33 Langmead, B. & Salzberg, S. L. Fast gapped-read alignment with Bowtie 2. *Nature methods* **9**, 357-359, doi:10.1038/nmeth.1923 (2012).

34 Zhang, Y. *et al.* Model-based analysis of ChIP-Seq (MACS). *Genome Biol* **9**, R137, doi:10.1186/gb-2008-9-9-r137 (2008).

35 Robinson, J. T. *et al.* Integrative genomics viewer. *Nat Biotechnol* **29**, 24-26, doi:10.1038/nbt.1754 (2011).

36 Durant, L. *et al.* Diverse targets of the transcription factor STAT3 contribute to T cell pathogenicity and homeostasis. *Immunity* **32**, 605-615, doi:10.1016/j.immuni.2010.05.003 (2010).

37 Ritchie, M. E. *et al.* limma powers differential expression analyses for RNA-sequencing and microarray studies. *Nucleic Acids Res* **43**, e47, doi:10.1093/nar/gkv007 (2015).

38 Wei, G. *et al.* Global mapping of H3K4me3 and H3K27me3 reveals specificity and plasticity in lineage fate determination of differentiating CD4+ T cells. *Immunity* **30**, 155-167, doi:10.1016/j.immuni.2008.12.009 (2009).

1071 39 Yusuf, I. *et al.* Germinal center T follicular helper cell IL-4 production is dependent on signaling
1072 lymphocytic activation molecule receptor (CD150). *Journal of immunology* **185**, 190-202,
1073 doi:10.4049/jimmunol.0903505 (2010).
1074 40 Suino, K. *et al.* The nuclear xenobiotic receptor CAR: structural determinants of constitutive
1075 activation and heterodimerization. *Mol Cell* **16**, 893-905, doi:10.1016/j.molcel.2004.11.036
1076 (2004).

Figure 1

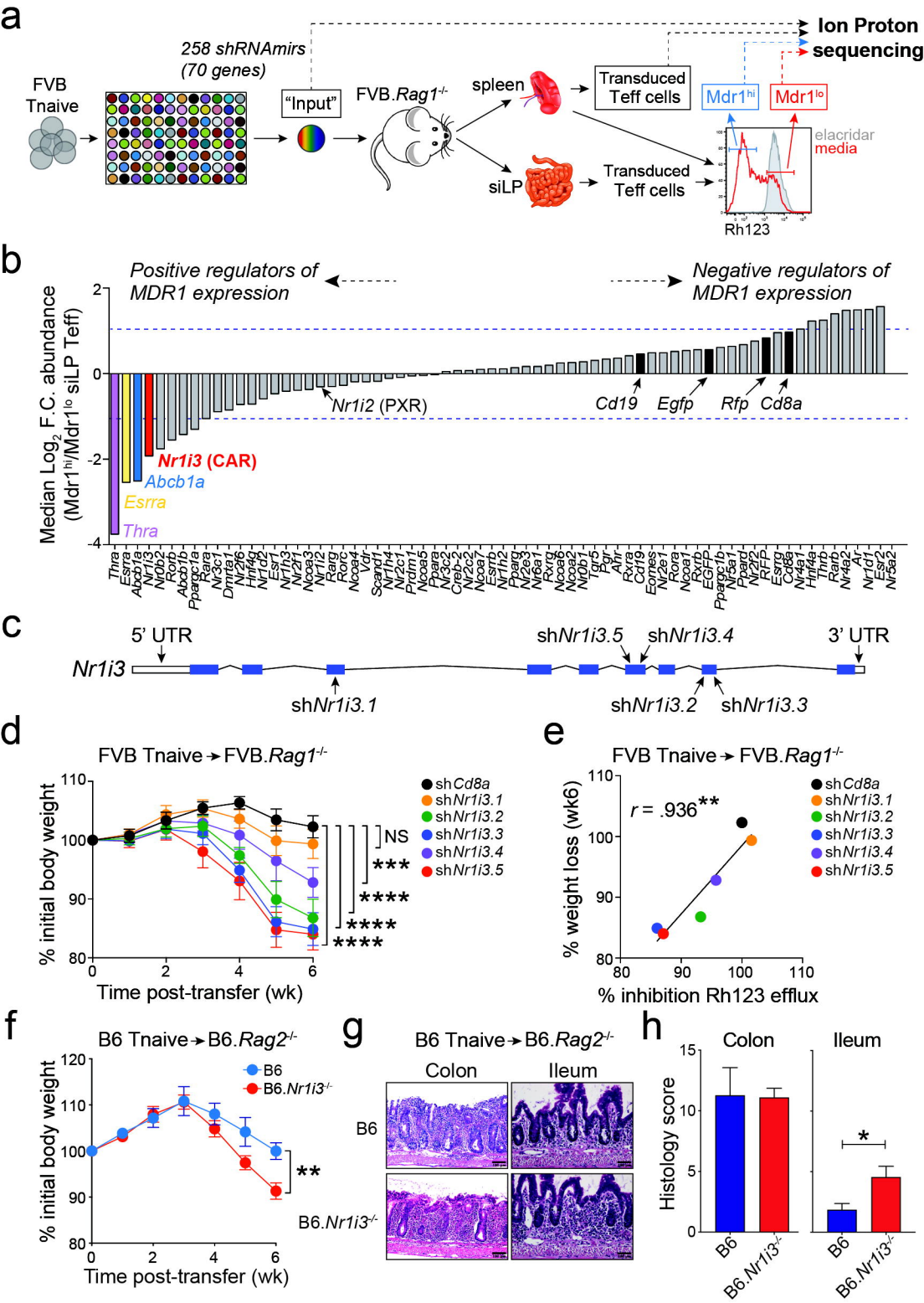
a
Ion Proton sequencing
258 shRNAmirs (70 genes)
FVB Tnaive
"Input"
FVB.Rag1-/-
spleen
siLP
Transduced Teff cells
Transduced Teff cells
Mdr1hi
Mdr1lo
elacridar
media
Rh123
b
Positive regulators of MDR1 expression
Negative regulators of MDR1 expression
Median Log2 F.C. abundance (Mdr1hi/Mdr1lo siLP Teff)
Nr1i2 (PXR)
Cd19
Egfp
Rfp
Cd8a
Nr1i3 (CAR)
Abcb1a
Esrra
Thra
c
5' UTR
3' UTR
Nr1i3
shNr1i3.1
shNr1i3.5
shNr1i3.4
shNr1i3.2
shNr1i3.3
d
FVB Tnaive → FVB.Rag1-/-
% initial body weight
Time post-transfer (wk)
shCd8a
shNr1i3.1
shNr1i3.2
shNr1i3.3
shNr1i3.4
shNr1i3.5
NS
***
****
****
****
e
FVB Tnaive → FVB.Rag1-/-
r = .936**
% weight loss (wk6)
% inhibition Rh123 efflux
f
B6 Tnaive → B6.Rag2-/-
B6
B6.Nr1i3-/-
**
% initial body weight
Time post-transfer (wk)
g
B6 Tnaive → B6.Rag2-/-
Colon
Ileum
B6
B6.Nr1i3-/-
h
Colon
Ileum
Histology score
*
B6
B6.Nr1i3-/-

Figure 2

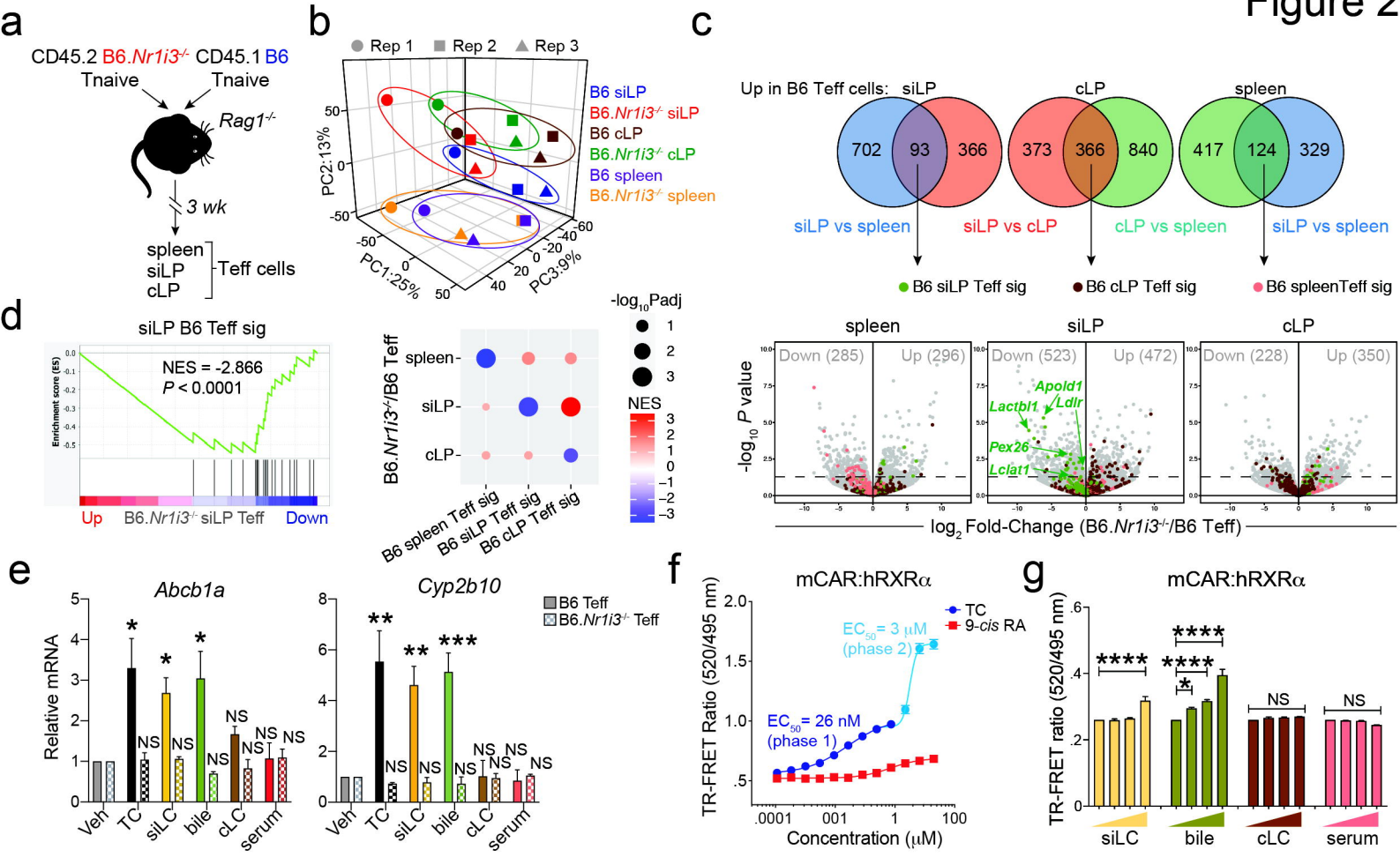
a
CD45.2 B6.Nr1i3-/- CD45.1 B6
Tnaive
Tnaive
Rag1-/-
3 wk
spleen
siLP
cLP
Teff cells
b
Rep 1
Rep 2
Rep 3
B6 siLP
B6.Nr1i3-/- siLP
B6 cLP
B6.Nr1i3-/- cLP
B6 spleen
B6.Nr1i3-/- spleen
PC2:13%
PC1:25%
PC3:9%
c
Up in B6 Teff cells:
siLP
cLP
spleen
702
93
366
373
366
840
417
124
329
siLP vs spleen
siLP vs cLP
cLP vs spleen
siLP vs spleen
B6 siLP Teff sig
B6 cLP Teff sig
B6 spleenTeff sig
spleen
siLP
cLP
Down (285)
Up (296)
Down (523)
Up (472)
Down (228)
Up (350)
Apold1
Lactbl1
Ldlr
Pex26
Lclat1
-log10 P value
log2 Fold-Change (B6.Nr1i3-/-/B6 Teff)
d
siLP B6 Teff sig
NES = -2.866
P < 0.0001
Enrichment score (ES)
Up
B6.Nr1i3-/- siLP Teff
Down
B6.Nr1i3-/-/B6 Teff
spleen
siLP
cLP
B6 spleen Teff sig
B6 siLP Teff sig
B6 cLP Teff sig
-log10Padj
NES
e
Abcb1a
Cyp2b10
B6 Teff
B6.Nr1i3-/- Teff
Relative mRNA
Veh
TC
siLC
bile
cLC
serum
NS
f
mCAR:hRXRα
TC
9-cis RA
EC50= 3 μM
(phase 2)
EC50= 26 nM
(phase 1)
TR-FRET Ratio (520/495 nm)
Concentration (μM)
g
mCAR:hRXRα
TR-FRET ratio (520/495 nm)
siLC
bile
cLC
serum
NS

Figure 3

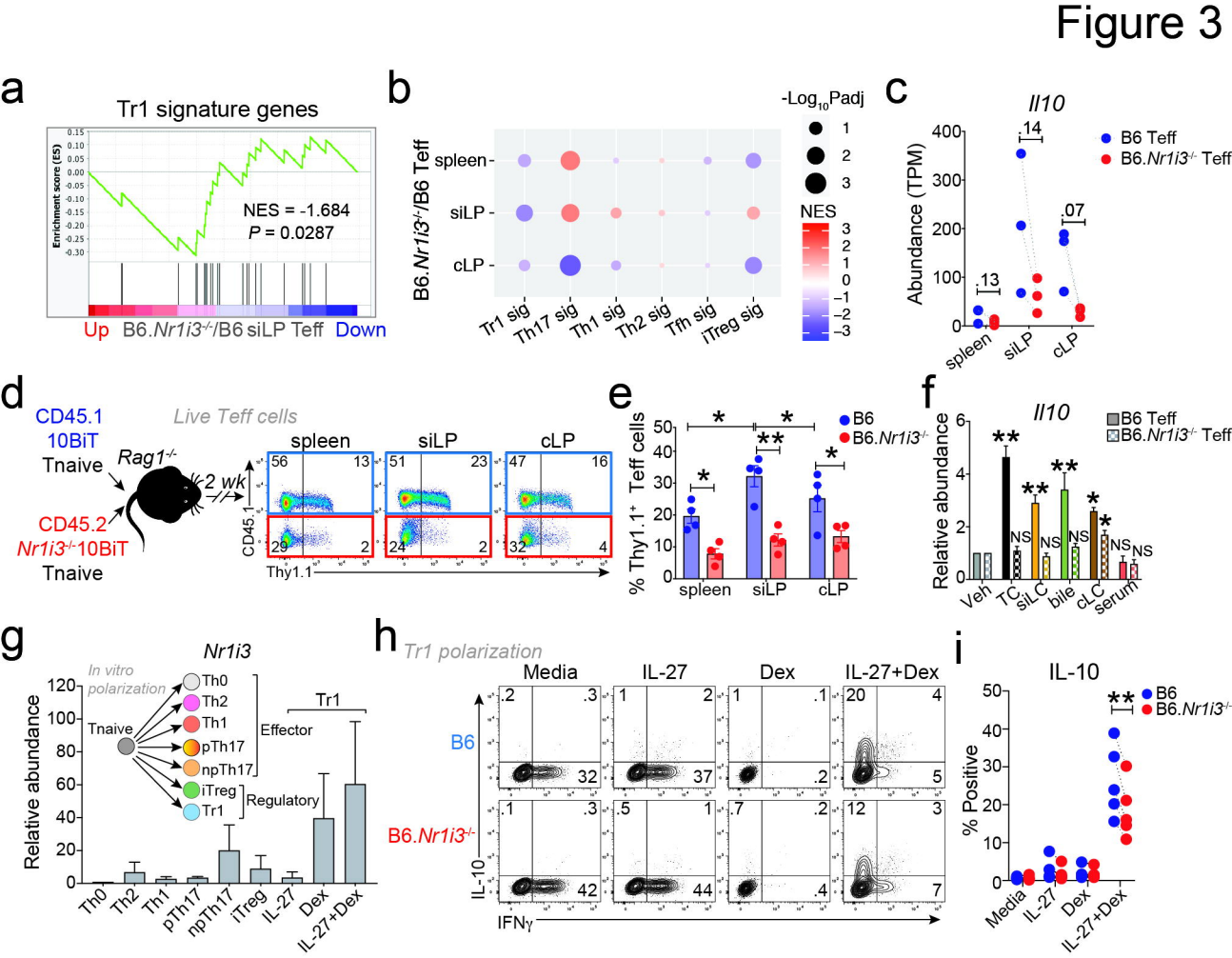
a
Tr1 signature genes
Enrichment score (ES)
NES = -1.684
P = 0.0287
Up
B6.Nr1i3-/-/B6 siLP Teff
Down
b
B6.Nr1i3-/-/B6 Teff
spleen
siLP
cLP
Tr1 sig
Th17 sig
Th1 sig
Th2 sig
Tfh sig
iTreg sig
-Log10Padj
NES
c
Il10
Abundance (TPM)
B6 Teff
B6.Nr1i3-/- Teff
.14
.13
.07
spleen
siLP
cLP
d
CD45.1
10BiT
Tnaive
Rag1-/-
2 wk
CD45.2
Nr1i3-/-10BiT
Tnaive
Live Teff cells
spleen
siLP
cLP
CD45.1
Thy1.1
56
13
29
2
51
23
24
2
47
16
32
4
e
% Thy1.1+ Teff cells
B6
B6.Nr1i3-/-
spleen
siLP
cLP
f
Il10
Relative abundance
B6 Teff
B6.Nr1i3-/- Teff
Veh
TC
siLC
bile
cLC
serum
NS
g
Nr1i3
In vitro polarization
Tnaive
Th0
Th2
Th1
pTh17
npTh17
iTreg
Tr1
Effector
Regulatory
Tr1
Relative abundance
Th0
Th2
Th1
pTh17
npTh17
iTreg
IL-27
Dex
IL-27+Dex
h
Tr1 polarization
Media
IL-27
Dex
IL-27+Dex
B6
B6.Nr1i3-/-
IL-10
IFNγ
.2
.3
32
1
2
37
1
.1
.2
20
4
5
.1
.3
42
.5
1
44
.7
.2
.4
12
3
7
i
IL-10
% Positive
B6
B6.Nr1i3-/-
Media
IL-27
Dex
IL-27+Dex

Figure 4

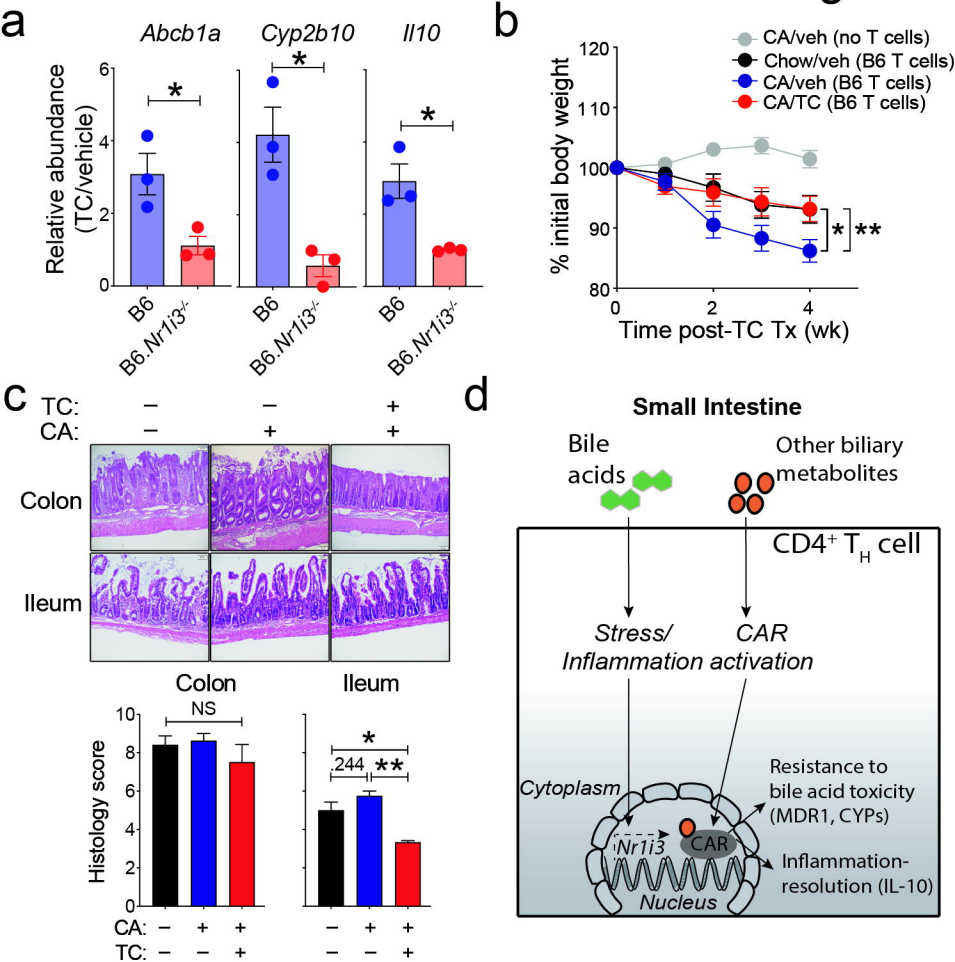
a
Abcb1a
Cyp2b10
Il10
Relative abundance (TC/vehicle)
B6
B6.Nr1i3-/-
b
CA/veh (no T cells)
Chow/veh (B6 T cells)
CA/veh (B6 T cells)
CA/TC (B6 T cells)
% initial body weight
Time post-TC Tx (wk)
c
TC:
CA:
Colon
Ileum
Histology score
NS
244
d
Small Intestine
Bile acids
Other biliary metabolites
CD4+ TH cell
Stress/ Inflammation activation
CAR
Cytoplasm
Nr1i3
Nucleus
Resistance to bile acid toxicity (MDR1, CYPs)
Inflammation-resolution (IL-10)